Membrane Fusion: Stalk Model Revisited

Vladislav S. Markin* and Joseph P. Albanesi†
*Department of Anesthesiology and †Department of Pharmacology, University of Texas Southwestern, Dallas, Texas 75390 USA

ABSTRACT Membrane fusion is believed to proceed via intermediate structures called stalks. Mathematical analysis of the stalk provided the elastic energy involved in this structure and predicted the possible evolution of the overall process, but the energies predicted by the original model were suspiciously high. This was due to an erroneous assumption, i.e., that the stalk has a figure of revolution of a circular arc. Here we abandon this assumption and calculate the correct shape of the stalk. We find that it can be made completely stress free and, hence, its energy, instead of being positive and high can become negative, thus facilitating the fusion process. Based on our new calculations, the energies of hemifusion, of complete fusion, and of the pore in a bilayer were analyzed. Implications for membrane fusion and lipid phase transitions are discussed.

INTRODUCTION

Membrane fusion plays a fundamental role in cell physiology. It is even believed to be a key event in the origin of life (Norris and Raine, 1998). For this reason it has attracted the intense interest of numerous researchers who have attempted to develop a model of this process (see Reviews and References therein, Chernomordik et al., 1995b; Jahn and Sudhof, 1999; Zimmerberg and Chernomordik, 1999; Burger, 2000; Stegmann, 2000; Melikyan et al., 2000). Both biological and artificial membrane fusion involves the merger of two phospholipid bilayers in an aqueous environment. In the early 1980s a qualitative picture of this process emerged suggesting that fusion proceeds via local contact between two lipid bilayers. Hui et al. (1981) termed this contact "a point defect" and proposed that it represented an intermediate stage of fusion. It was clear that membranes could not expose their hydrophobic interiors to water (reflected by Gingel's famous statement: "membranes hate edges." And he went on: "All our ideas of membrane transformations are based on this fact") (Gingell and Ginsberg, 1978). Therefore, to make a connection between two membranes, their monolayers must be strongly bent into an hourglass shape. This structure was called a stalk, and the whole mechanism was called the stalk model. Its mathematical analysis was performed in 1983 (Kozlov and Markin, 1983) with the first English publication appearing in 1984 (Markin et al., 1984).

Mathematical implementation of the stalk model was based on calculation of the elastic energy of the curved monolayers and elucidation of the chain of events leading either to complete fusion or to abortion of the process. The model proved to be very attractive and was adopted in numerous studies, both experimental and theoretical (Leikin et al., 1987; Kozlov et al., 1989; Nanavati et al., 1992; Siegel, 1993; Chizmadzhev et al., 1995, 1999, 2000; Siegel, 1999; Kuzmin et al., 2001). Its success was based on its ability to explain a number of experimental observations (Monck and Fernandez, 1994; Chernomordik et al., 1995a,b, 1997; Chernomordik, 1996; Melikyan et al., 1997; Basanez et al., 1998; Lee and Lentz, 1998; Zimmerberg and Chernomordik, 1999; Goni and Alonso, 2000; Razinkov and Cohen, 2000). Later on the model was further developed to include additional features such as hydrophobic voids (Siegel, 1993), fusion pore dilatation in stages (Chizmadzhev et al., 1995), relative sliding of monolayers (Chizmadzhev et al., 1999), role of membrane tension (Nanavati et al., 1992; Chizmadzhev et al., 2000), et cetera.

However, all these papers had to deal with one significant difficulty: because of the high curvature of the stalk, the calculation of its elastic energy inevitably resulted in very high values, up to hundreds kT. D. Siegel wrote in 1999, "It is troubling that energies predicted for stalk and transmonolayer contact (TMC) intermediates are so high." This energy is too high and raises doubts on the feasibility of the whole model. From the very beginning (1983, 1984) significant efforts were spent in finding a way for the stalk to decrease its energy. The obvious factor to consider was the spontaneous curvature of lipid monolayers. This helped to some extent but at the expense of a necessitating assumption of very high spontaneous curvature at the limit of reasonable values. This struggle with the high bending energy of the stalk continues to this day, sometimes eliciting very ingenious ideas and suggestive terminology (Kuzmin et al., 2001).

This stalk paradox is rather disturbing: the model seems to be intuitively reasonable and agrees with experimental observations, but it suffers from inherent difficulty. We believe that the resolution of this paradox should be found within the stalk model proper rather than by enlisting additional and sometimes artificial considerations. To this end we performed an analysis of the

Submitted October 16, 2001, and accepted for publication November 16, 2001.

Address reprint requests to Vladislav S. Markin, Department of Anesthesiology, UT Southwestern, Dallas, TX 75390-9068. Tel.: 214-648-5632; Fax: 214-648-6799; E-mail: vladislav.markin@utsouthwestern.edu.

© 2002 by the Biophysical Society

0006-3495/02/02/693/20 $2.00

stalk model ab initio. We found that with the correct mathematical treatment of the model all of the difficulties researchers had been struggling with disappeared. Indeed, these difficulties were simply the result of a single unjustified assumption in the stalk model.

The source of these apparent difficulties is the shape of the stalk. Since the original papers (Kozlov and Markin, 1983) the shape of the stalk was not calculated but rather postulated to be the figure of revolution of a circular arc. It was this postulate that brought about a very high bending energy of the stalk. So, following Zimmerberg (2000), we asked the same question: "Are the curves in all the right places?" As we now report, with the right shape of this intermediate structure the stalk can be made completely stress free and its bending energy reduced to zero or even to negative values.

Thus, the numerical results of the original paper (Kozlov and Markin, 1983) are not valid for the properly shaped stalk. Unfortunately, all subsequent theoretical papers devoted to the stalk model followed the lead without questioning the postulate of circular shape. Therefore their conclusions regarding the high bending energy are also wrong. One of us (V.S.M.) is personally responsible for this unjustified assumption and we feel obligated to correct this inaccuracy in the stalk analysis.

THEORETICAL

Original stalk model

In the original model of 1983 (Kozlov and Markin, 1983) the stalk was visualized as an hourglass-shaped local connection between two membranes. It could be comprised of one or two monolayers of opposing membranes, producing either a monolayer or bilayer stalk. Later the monolayer stalk was accepted as a key intermediate in the overall fusion process known as a hemifusion stage, and the bilayer stalk was baptized a fusion pore. The stalk could form after direct closure upon one another of two bulging defects in opposing membranes (layers) having initial curvature, c_{init}, and a spontaneous curvature, c_0.

It was assumed that the stalk and surrounding membranes form an axisymmetrical body of revolution (Fig. 1) with the neutral surface (dotted line) drawn somewhere in the middle of the layer transformed into the stalk. Here a is the shortest distance from the neutral surface to the axis of revolution, r is the marginal radius of the stalk, b is the distance from the axis of revolution to the point where the branches of the stalk become horizontal. Parameters a and b could be called the neck and the width of the stalk. In the original version of the model $b = a + r$. The coordinates of the contour are x and z, and the angle between the contour and horizontal line is ψ.

According to Helfrich (1973), the density of bending energy accumulated in the stalk is given as

$$w = \frac{\kappa}{2}(c_{\text{m}} + c_{\text{p}} - c_0)^2 \tag{1}$$

in which κ is bending rigidity and c_{m} and c_{p} are principal curvatures along the meridian and parallel to the body of revolution representing the stalk. The energy associated with Gaussian curvature was neglected as it became customary in all subsequent papers. The energy of the stalk was defined as its elastic energy minus the initial elastic energy of two layers without stalks:

$$W_{\text{s}} = \pi\kappa\left[\int_{\text{stalk}} dA(c_{\text{m}} + c_{\text{p}} - c_0)^2 - \int_{\text{stalk}} dA(c_{\text{init}} - c_0)^2\right] \tag{2}$$

The integrals are taken over the total surface of the stalk. The first integral represents the bending energy of the stalk membrane and the second integral is equal to the bending energy of the initial membrane. The stalk energy W_{s} was found to be

$$W_{\text{s}}(a, r) = 2\pi\kappa\left\{\left[\left(\frac{2}{r} + c_0\right)^2 - (2c_{\text{init}} - c_0)^2\right] \times \left[\frac{\pi}{2}r(r + a) - r^2\right] - \pi\left(\frac{2}{r} + c_0\right)(r + a) + \frac{2(r + a)^2}{r\sqrt{a(2r + a)}}\arctan\sqrt{\frac{2r + a}{a}}\right\}. \tag{3}$$

If the fusing membranes initially were planar, $c_{\text{init}} = 0$, then

$$W_{\text{s}}(a, r) = 2\pi\kappa\left[-4 - rc_0(4 - \pi) + \pi ac_0 + \frac{2(r + a)^2}{r\sqrt{a(2r + a)}}\arctan\sqrt{\frac{2r}{a} + 1}\right] \tag{4}$$

In the absence on spontaneous curvature ($c_0 = 0$), the bending energy depends only on the ratio r/a; the function has the minimum equal to $E_{\text{min}} = 3.791\ \kappa$, which occurs at $r/a = 1.671$. Final results depend on the value of the bending rigidity. Chizmadzhev et al. (1995) assumed that bilayer rigidity equals $\sim 10^{-19}$ J, giving the minimum monolayer stalk energy of $E_{\text{min}} = 45.5$ kT. If, as more often assumed, $\kappa \cong 10\ kT$, the minimum energy of the stalk is 37 kT.

If spontaneous curvature of the bent layer is not zero, then its energy depends on the variables r and a separately. The initial

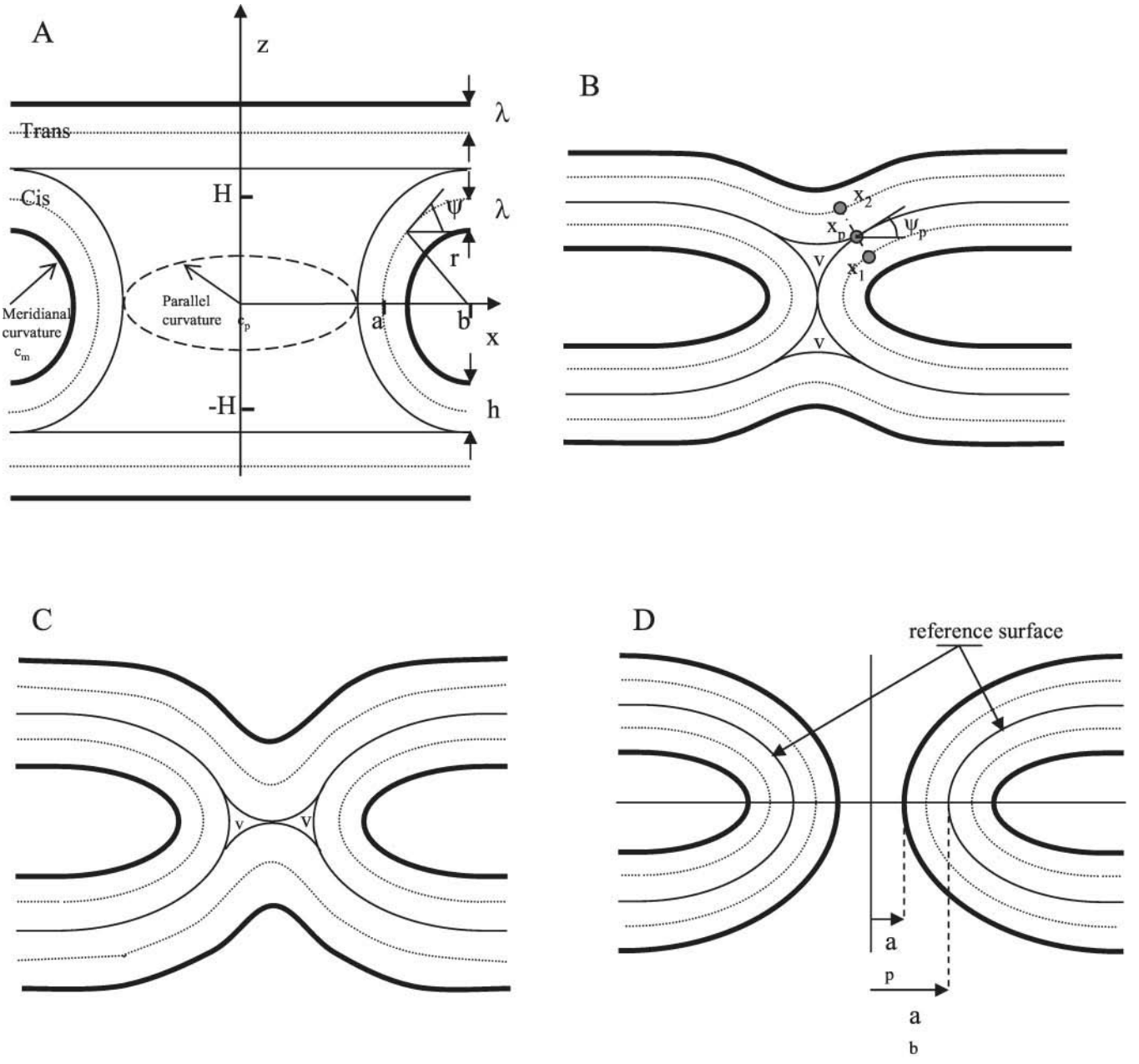

FIGURE 1 Steps in membrane fusion. Solid lines represent hydrophilic surfaces, thin lines represent hydrophobic, dotted lines represent neutral surfaces. (*A*) Parameters of the stalk. (*B*) Hemifusion, initial stage. (*C*) Hemifusion, transmonolayers contact. (*D*) Complete fusion—fusion pore.

monolayer stalk has $a \approx 1$ nm. For $c_0 = -0.01$ nm^{-1} the minimal energy of 3.68, $\kappa \approx 44.2\ kT$ occurs at $r = 1.66$ nm. For $c_0 = -0.1$ nm^{-1} the minimal energy of 2.68 $\kappa \approx 32\ kT$ occurs at $r = 1.54$ nm.

Stress-free stalk

Now we shall no longer make the assumption that the stalk is circular in shape but instead its shape will be calculated. Therefore in Fig. 1 *A* parameter r should be disregarded and the stalk is considered to be a figure of revolution of a certain arbitrary curve. In this curve a is its shortest distance from the axis of revolution, b is the point where the stalk smoothly connects with the rest of the planar membrane. For simplicity, the initial membranes are considered planar. $2H$ is the distance between neutral surfaces of fusing layers. The contour is supposed to be smooth, and no sharp points are allowed.

The principal curvatures of the stalk (Deuling and Helfrich, 1977; Volkov et al., 1998; Markin et al., 1999) are given by equations

$$c_p(x) = \frac{\sin \psi(x)}{x}; \quad c_m(x) = \cos \psi(x) \frac{d\psi}{dx} \tag{5}$$

To find the stress-free stalk we impose the condition that the total curvature of the stalk is constant and equal to c_{stalk}:

$$c_p(x) + c_m(x) = c_{stalk} \tag{6}$$

If $c_{stalk} = c_0$, the stalk is stress free.

This approach was used previously for the analysis of myelin shapes (Deuling and Helfrich, 1977) and beading of nerve fibers under lateral tension (Markin et al., 1999). The contour of the stalk neutral surface can be presented (Volkov et al., 1998; Markin et al., 1999) as

$$\frac{dz}{dx} = \tan \psi(x) = \frac{xc_p}{\sqrt{1 - x^2c_p^2}} \tag{7}$$

For the contour in Fig. 2, one can find from Eq. 5 that

$$xc_p = \frac{1}{2} c_{stalk}x + \frac{a}{x}\left(1 - \frac{1}{2} c_{stalk}a\right) \tag{8}$$

Then the final equation for the contour takes the form

$$\frac{dz}{dx} = \left\{\left[\frac{1}{2} c_{stalk}x + \frac{a}{x}\left(1 - \frac{1}{2} c_{stalk}a\right)\right]^{-2} - 1\right\}^{-1/2} \tag{9}$$

Parameter b of the stalk can be found from the condition $dz/dx = 0$; then

$$b = \sqrt{a^2 - \frac{2a}{c_{stalk}}}, \quad \text{or} \quad \frac{b}{a} = \sqrt{1 - \frac{2}{ac_{stalk}}} \tag{10}$$

The last equation shows that the ratio b/a depends on a single dimensionless parameter ac_{stalk}. The same is true for the shape of the stalk $z = z(x)$ given by the following equation:

$$\frac{z}{a} = \int_1^{x/a} \left\{\left[\frac{1}{2} ac_{stalk}\, t + \frac{1}{t}\left(1 - \frac{1}{2} ac_{stalk}\right)\right]^{-2} - 1\right\}^{-1/2} dt \tag{11}$$

As one can see from here, the shape of the stalk is indeed determined by a single parameter ac_{stalk} because the upper limit of this integral b/a is also a function of the same parameter according to Eq. 10. In Fig. 2 *A* we presented the contour of the stalk neutral surface with parameters $ac_{stalk} = -0.1$. One can see that the contour of the stalk is not a circular arc and that its branches at the end become horizontal. The important point is that if $c_{stalk} = c_0$, then this stalk is completely stress free because its total curvature at every point is equal to the spontaneous curvature c_0. Fig. 2 *B* gives a three-dimensional view of that stalk (of its neutral surface).

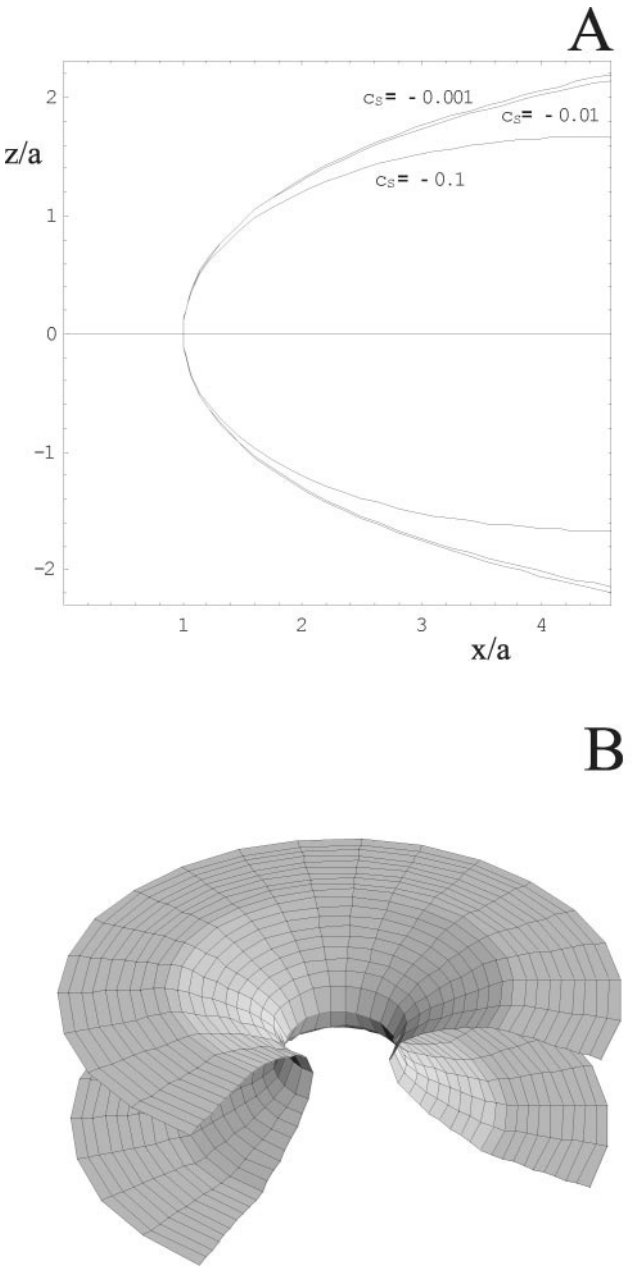

FIGURE 2 Stress-free stalk. (*A*) Two-dimensional contours for three different spontaneous curvatures shown in the graph. (*B*) Three-dimensional rendition of the stalk with $c_0 = -0.1$ nm^{-1}.

The height of the stalk $L = 2H$ is found from the integral (Eq. 11) with $x = b$. In the absence of an analytical solution for the stress free stalk (Eq. 11) it is useful to have a good approximation for it. From the analysis of series expansion of (Eq. 11)

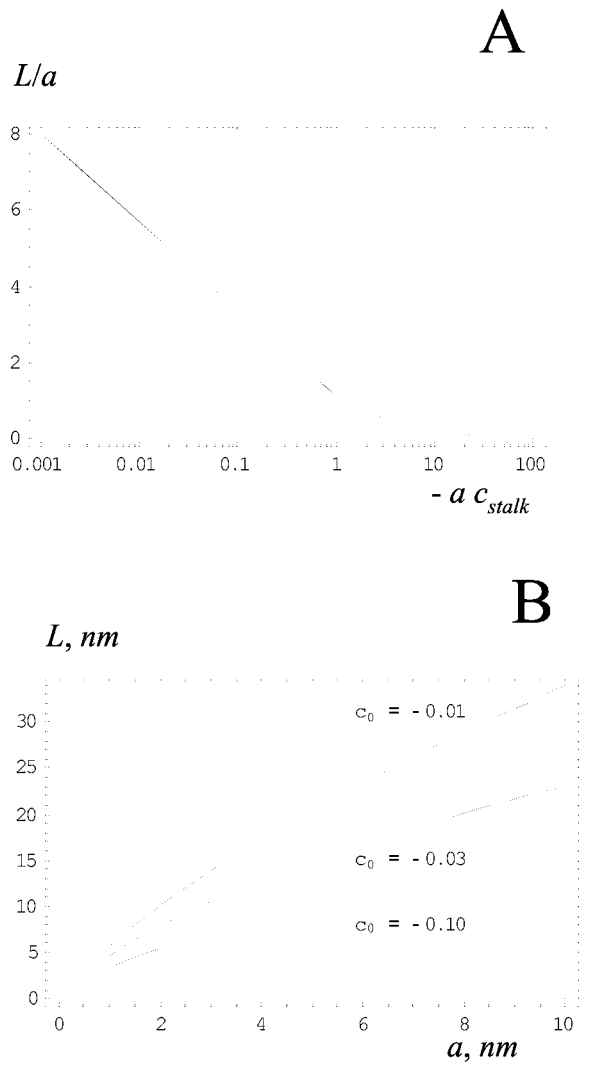

FIGURE 3 Parameters of the stress-free stalk. (*A*) Normalized height of the stalk L/a as the function of $-ac_{\text{stalk}}$. (*B*) Height of the stalk L as a function of the neck radius a for different values of spontaneous curvature c_{stalk} shown at the curves in nm^{-1}.

at points $x = a$ and $x = b$ one can find a piece-wise approximating function for L:

$$\frac{L}{a} = \frac{2}{0.68435 - ac_{\text{stalk}}}, \quad \text{if} \quad ac_{\text{stalk}} < -1 \tag{12a}$$

and

$$\frac{L}{a} = 0.6384 \log[1 + 5.4245(-ac_{\text{stalk}})^{-1.5666}], \quad \text{if} \quad ac_{\text{stalk}} > -1 \tag{12b}$$

Notice that the dimensionless normalized distance L/a depends on a single parameter, ac_{stalk}, only. This function is presented in Fig. 3 *A* together with a numerical solution (Eq. 11). Two lines are indistinguishable at this resolution demonstrating that function (Eq. 12) closely approximates the distance between fusing membranes. Practically, one cannot expect that ac_{stalk} would reach a high negative value. Therefore we need only the values between -1 and -0.001, given by Eq. 12b. Hence the distance between membranes (neutral surfaces) is given by

$$L = 2H = 0.6384\, a \log\lfloor 1 + 5.4245(-ac_{\text{stalk}})^{-1.5666}\rfloor \tag{13}$$

Notice, that this relationship does not depend on membrane stiffness κ.

Equation 12 and the resulting plot in Fig. 3 *A* have universal character applicable at any (negative) spontaneous curvature. However, for practical purposes a dimensional Eq. 13, illustrated in Fig. 3 *B* for a few selected values of c_0, is more convenient.

Stalk energy

Now let us determine the energy of the stalk. Because the curvature of the stalk is constant and equal to c_{stalk}, its bending energy is $\frac{1}{2}\kappa(c_{\text{stalk}} - c_0)^2 A$, in which A is the area of the stalk. If $c_{\text{stalk}} = c_0$, bending energy is zero. We have to subtract from here the initial energy of the membrane in the planar state if spontaneous curvature is not zero. In the planar state fusing layers have elastic energy equal to $\frac{1}{2}\kappa c_0^2 A$. Therefore the energy of the stalk is

$$W_s = \tfrac{1}{2}\kappa A[(c_{\text{stalk}} - c_0)^2 - c_0^2] \tag{14}$$

Notice that the energy of the stress free stalk is $-\frac{1}{2}\kappa c_0^2 A$ and it is negative. To complete this calculation we have to find stalk area A. If the infinitesimal length of the contour in Fig. 1 A is $dl = dx/\cos\psi$, the differential of the area can be found as

$$dA = 2\pi x\, dl = \frac{2\pi x\, dx}{\cos\psi} = 2\pi x\, dx\sqrt{1 + \left(\frac{dz}{dx}\right)^2} = \frac{2\pi\, x\, dx}{\sqrt{1 - \left[\frac{1}{2}c_{\text{stalk}}x + \frac{a}{x}\left(1 - \frac{1}{2}c_{\text{stalk}}a\right)\right]^2}} \tag{15}$$

And hence

$$A = 4\pi\int_a^b \frac{x\, dx}{\sqrt{1 - \left[\frac{1}{2}c_{\text{stalk}}x + \frac{a}{x}\left(1 - \frac{1}{2}c_{\text{stalk}}a\right)\right]^2}} \tag{16}$$

Now the total energy of the stalk can be presented as

$$W_s = 2\pi\kappa\int_1^{b/a} \frac{\lfloor (ac_{\text{stalk}} - ac_0)^2 - ac_0^2\rfloor t\, dt}{\sqrt{1 - \left[\frac{1}{2}ac_{\text{stalk}}t + \frac{1}{t}\left(1 - \frac{1}{2}ac_{\text{stalk}}\right)\right]^2}} \tag{17}$$

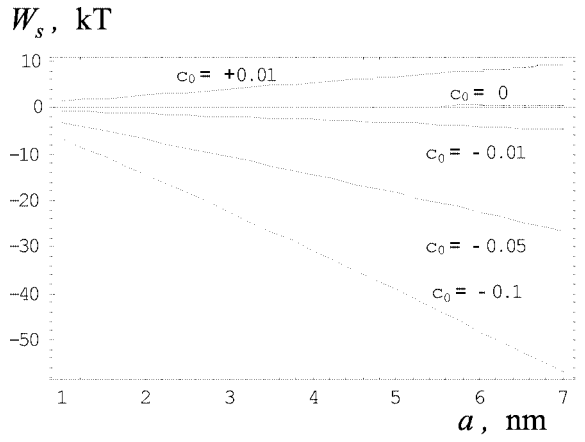

FIGURE 4 Bending energy of the stress-free stalk with different c_0 shown at the curves in nm^{-1} as a function of its radius a (below abscissa). Above abscissa there are two curves with zero or small positive spontaneous curvature; these stalks are not stress free, however, their bending energy is very small.

The dependence of the stalk energy on its radius a is presented in Fig. 4 for different values of spontaneous curvature c_0. As one can conclude from here, the stalk has negative energy, it tends to expand and to push away fusing membranes. For comparison with previous results we present in Table 1 the energy of the initial monolayer stalk (a_{stalk} = 1 nm) both for the old model and the new one in units of kT. One can see a huge difference between the two models.

Hemifusion

Let us consider the initial hemifusion structure presented in Fig. 1 *B*. At some point *P* the *trans* monolayer peels off of the *cis* monolayer. Let this point have coordinate x_p and angle $\psi = \psi_p$. Designate the corresponding points at the neutral surfaces of *cis* and *trans* monolayers x_1 and x_2. The surface between the two monolayers will be considered a reference surface and its curvature will be designated c^b. The whole structure can be divided into three parts: the "wings" of the hemi-fused bilayers beyond the point $x = x_1$, the "neck" of the stalk in the range $x < x_1$, and two dimples formed by *trans* monolayers in the range $x < x_2$. The monolayers of these three parts are smoothly connected to each other. The total energy of hemifusion

TABLE 1 Stalk energy

Curvature (c_0, nm^{-1})	Energy, kT units	
	Old Model	Stress Free Stalk
−0.001	+37.8	−1.20
−0.01	+36.8	−1.91
−0.1	+26.8	−6.87

W_h consists of the bending energy of the neck W_n, of the wings W_w, of the dimples W_d, and hydrophobic energy of two voids W_v. We shall calculate each of these components.

First, let us find coordinate x_1. If the stalk has curvature c_s and the neck radius a, then from Eqs. 5 and 8 one can find that

$$x_1 = \frac{\sin\psi_p - \sqrt{(\sin\psi_p)^2 - 2ac_s + a^2c_s^2}}{c_s} \tag{19}$$

and then

$$x_p = x_1 - (h - \lambda)\sin\psi_p,$$

and

$$x_2 = x_1 - 2(h - \lambda)\sin\psi_p. \tag{20}$$

The energy of the stalk neck W_{neck} can be readily found from Eq. 17 if the integral is taken from 1 to x_1/a.

Calculation of the energy of the wings W_w is more complicated. We select the interface between two monolayers as a reference surface, and coordinates of monolayer neutral surfaces will be related to this reference surface. As in the previous section, we assume that the reference surface has constant total curvature. This assumption will be discussed later. The principal curvatures c_m and c_p of the reference surface are defined the same way as for a monolayer stalk by Eq. 5. That means that $c_m < 0$ and $c_p > 0$. Designate λ the distance from the hydrophilic surface of a monolayer to its neutral surface. Then the principal curvatures of the *cis* monolayer are given by the equations

$$c_p^{cis} = \frac{c_p}{c_p(h - \lambda) + 1} \quad \text{and} \quad c_m^{cis} = \frac{c_m}{c_m(h - \lambda) + 1} \tag{21}$$

The curvatures of the *trans* monolayer have the opposite sign and can be presented as

$$c_p^{trans} = \frac{c_p}{c_p(h - \lambda) - 1}$$

and

$$c_m^{trans} = \frac{c_m}{c_m(h - \lambda) - 1} \tag{22}$$

Notice that these definitions are consistent for both monolayers. We "look" at a monolayer from the aqueous phase: if the monolayer in a given principal plane is convex, then this curvature is positive and vice versa. The geometry of the wings of the hemi-fused bilayer is determined by a set of three parameters: x_p, ψ_p, and c^b.

One can find that the principal curvatures of the reference surface of the hemi-fused bilayer are given by

$$c_p = \frac{1}{2}c^b + \frac{x_p}{x^2}\left(\sin\psi_p - \frac{1}{2}c^b x_p\right)$$

and

$$c_m = \frac{1}{2}c^b - \frac{x_p}{x^2}\left(\sin\psi_p - \frac{1}{2}c^b x_p\right) \quad (23)$$

Instead of Eq. 10 the length of the wings is given by

$$b_w = \sqrt{x_p^2 - \frac{2x_p\sin\psi_p}{c^b}} \quad (24)$$

and the area differential is

$$dA = \frac{2\pi\, x\, dx}{\sqrt{1 - \left[\frac{1}{2}c^b x + \frac{x_p}{x}\left(\sin\psi_p - \frac{1}{2}c^b x_p\right)\right]^2}} \quad (25)$$

The bending energy density of the bilayer wings, referred to its reference surface, can be presented as

$$w_w = \frac{\kappa}{2}\left\{\left[\left(\frac{2(h-\lambda)c_m c_p + c_m + c_p}{(c_m(h-\lambda)+1)(c_p(h-\lambda)+1)} - c_0^{cis}\right)^2 - (c_0^{cis})^2\right]\left[1 + (c_m + c_p)(h-\lambda) + c_m c_p (h-\lambda)^2\right] + \left[\left(\frac{2(h-\lambda)c_m c_p - c_m - c_p}{(c_m(h-\lambda)-1)(c_p(h-\lambda)-1)} - c_0^{trans}\right)^2 - (c_0^{trans})^2\right]\left[1 - (c_m + c_p)(h-\lambda) + c_m c_p (h-\lambda)^2\right]\right\} \quad (26)$$

in which c_0^{cis} is the spontaneous curvature of the *cis* monolayer and c_0^{trans} is the same for the *trans* monolayer.

The total free energy of the bilayer wings is given by the integral over the area of the reference surface from radius x_p to b_w:

$$W_w = \int w_w dA \quad (27)$$

To estimate the dimple energy we assume that it has a spherical shape. Its radius is $r_d = x_2/\sin\psi_p$, and hence the bending energy of two dimples is

$$W_d = 8\pi\kappa(1 - \cos\psi_p)(1 + r_c c_0^{trans}) \quad (28)$$

Total bending energy of the hemi-fused bilayers is

$$W_{hb} = W_n + W_w + W_d \quad (29)$$

For the sake of comparison with previous numerical results we assume that $\lambda = h/2 = 1$ nm, $\kappa = 10$ kT, and $\psi_p = \pi/6$. Suppose that monolayers have no spontaneous curvature. Then the stress free stalk neck does not contribute any energy to Eq. 26. Bilayer wings contribute $W_w = 2.8$ kT and dimples have $W_d = 33.7$ kT. Therefore in total bending energy of W_{hb} (36.5 kT) the main contribution comes from the dimples and constitutes approximately 92% of the total.

The presence of spontaneous curvature in monolayers helps to decrease the bending energy of hemifusion. For example, if c_0 of both monolayers is -0.1 nm^{-1} and $\psi_p = 30°$, then $W_n = -1.1$ kT, $W_w = -2.7$ kT, $W_d = 28.4$ kT, and the total is only $W_{hb} = 24.6$ kT.

The result strongly depends on where the monolayer peel-off occurs, i.e. what is the value of the peel-off angle. If it happens a little farther from the axis of the stalk then the bending energy drastically decreases. For example, if $\psi_p = 15°$ and there is no spontaneous curvature then $W_w = 0.1$ kT, $W_c = 8.4$ kT, and the total is only $W_{hb} = 8.5$ kT.

Finally, if the peel-off point occurs at $\psi_p = 15°$ and spontaneous curvature is $c_0 = -0.1$ nm^{-1}, then $W_n = -2.5$ kT, $W_w = -1.6$ kT, $W_c = 1.4$ kT, and the total becomes negative $W_{hb} = -2.7$ kT.

Therefore, the bending energy of the hemifused bilayers can be very low and even negative if the monolayers have rather pronounced spontaneous curvature. Fig. 5 *A* presents the bending energy of hemifusion as a function of peel-off angle for two types of bilayer: with no spontaneous curvature of monolayers and with $c_0 = -0.1$ nm^{-1}. As one can see, in the absence of spontaneous curvature the bending energy would be zero if $\psi_p = 0°$. This obviously means that the *trans* monolayer would prefer to remain planar. In the presence of spontaneous curvature $c_0 = -0.1$ nm^{-1} the bending energy would reach a minimum at $\psi_p = 5°$ and it would be negative at this configuration and equal to -8 kT.

The actual value of the peel off angle is determined by the minimum of the total free energy of the system including the bending energy and the energy of interstices at the stalk axis. It will be considered in the next section.

Hydrophobic voids

Siegel was the first to pay attention to the fact that at the ends of a monolayer stalk there should be void interstices (Markin and Hudspeth, 1993; Siegel, 1993) because three lipid monolayers meeting here cannot fit together without gaps. The shape of the interstices at the initial stage of hemifusion is presented in Fig. 6. The voids carry two additional contributions to the total energy of the system associated with their volume, V, and area, A:

$$W_{void} = W_{void,V} + W_{void,A} \quad (30)$$

Assuming that the void is nothing but vacuum, one can estimate the first term as

$$W_{void,V} = P_{atm} V. \quad (31)$$

in which P_{atm} is atmospheric pressure. However, 1 atm is equivalent to 0.025 kT/nm^3. Therefore even if the void

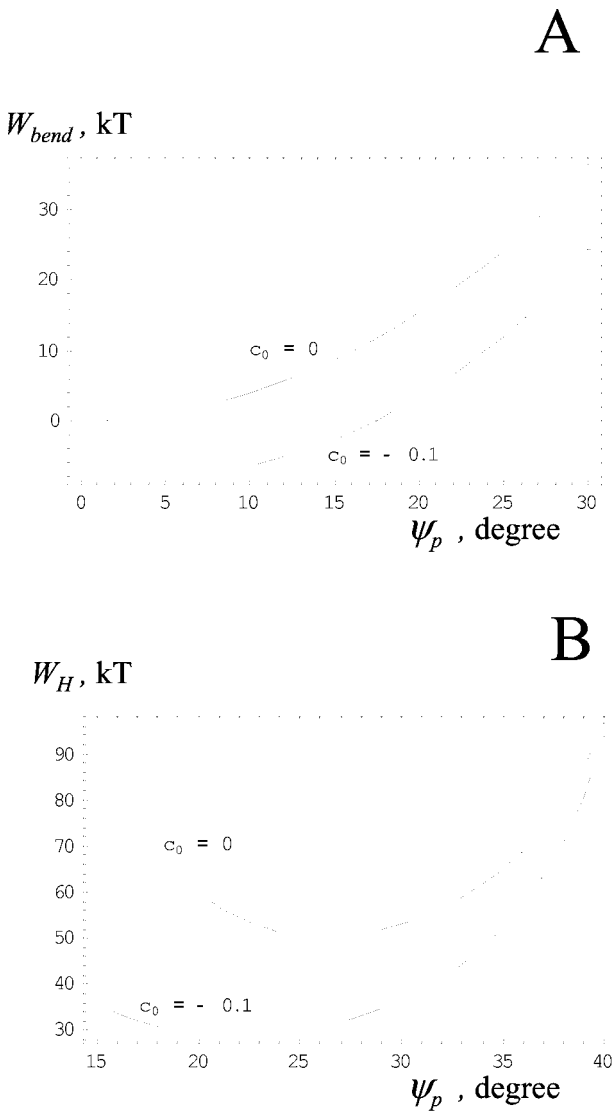

FIGURE 5 Free energy of the hemifusion as a function of peel-off angle ψ_p for two types of bilayer: with no spontaneous curvature and with $c_0 = -0.1$ nm^{-1}. (*A*) Bending energy only. (*B*) Total energy of hemifusion, $\gamma_{eff} = 1.9$ mN/m $= 0.48\ k_BT$/nm^2.

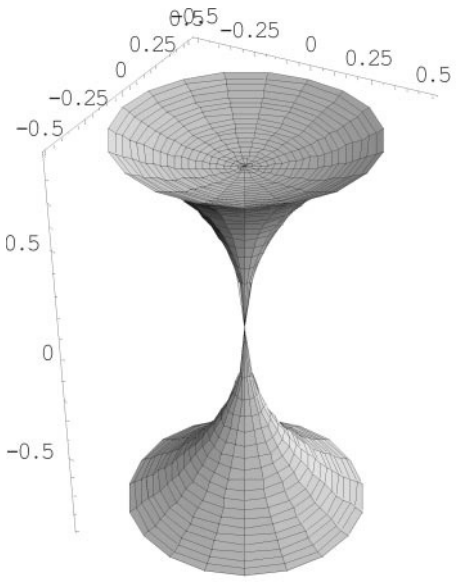

FIGURE 6 Shape of interstices at the initial stage of hemifusion.

volume amounts to a few dozens of nm^3 (and this is all we deal with in the stalk model), $W_{void,V}$ barely reaches 1 kT and hence can be safely neglected.

The hydrophobic energy of the void was initially estimated by Siegel in 1993 (Siegel, 1993) and subsequently corrected in 1999 (Siegel, 1999). The estimate was based on the assumption that the hydrophobic interstice surface is equivalent to the surface of long chain alkanes with vacuum, which is known to be in the range 20 to 27 mN/m. However, using these numbers to find the energy of interstices in the H_{II} phase one would come up with energy that is an order of magnitude higher than what is known for the H_{II} phase (Siegel, 1993). The reason is that much of the "surface area" of the interstice lies at the rim of the interstice, where two lipid/vacuum interfaces would be less than 0.1 nm apart. In this case one cannot use the surface tension of the free surface lest the energy be strongly overestimated. There are two solutions to this dilemma. One might try to take into consideration the existence of the other hydrophobic surface in close proximity and calculate the energy of two surfaces as the function of the distance between them. However, this path involves rather poorly known functions and in the complex geometry of interstices these calculations could give a very approximate result. One can of course try to approximate the interstice geometry with a simple geometrical shape, like a cylinder (Kuzmin et al., 2001), but this approach completely neglects the interstices at the initial stage of hemifusion (Fig. 6).

A different approach was proposed in Siegel (1999) that was based on surface area scaling. Siegel suggested using an "effective surface tension" and found it to be $\gamma_{eff} = 1.9$ mN/m $= 0.48\ k_BT$/nm^2. This approach seems quite reasonable and convenient in practical implementation. We shall use it below.

Based on the previous equations for the shape of *trans* and *cis* monolayers we calculated the area of voids A_{void} and found their hydrophobic energy $W_{void} = \gamma_{eff} A_{void}$. Total energy of the hemifusion is equal to

$$W_h = W_{hb} + W_{void} \tag{32}$$

and it is a function of the stalk radius a_s and peel-off angle ψ_p. Actual shape of the hemifusion structure is determined by interplay between bending energy and hydrophobic energy. At a given a_s angle ψ_p is determined by the minimum of the total energy.

Fig. 5 *B* presents the total energy of hemifusion as a function of peel-off angle for two cases: $c_0 = 0$ and $c_0 =$

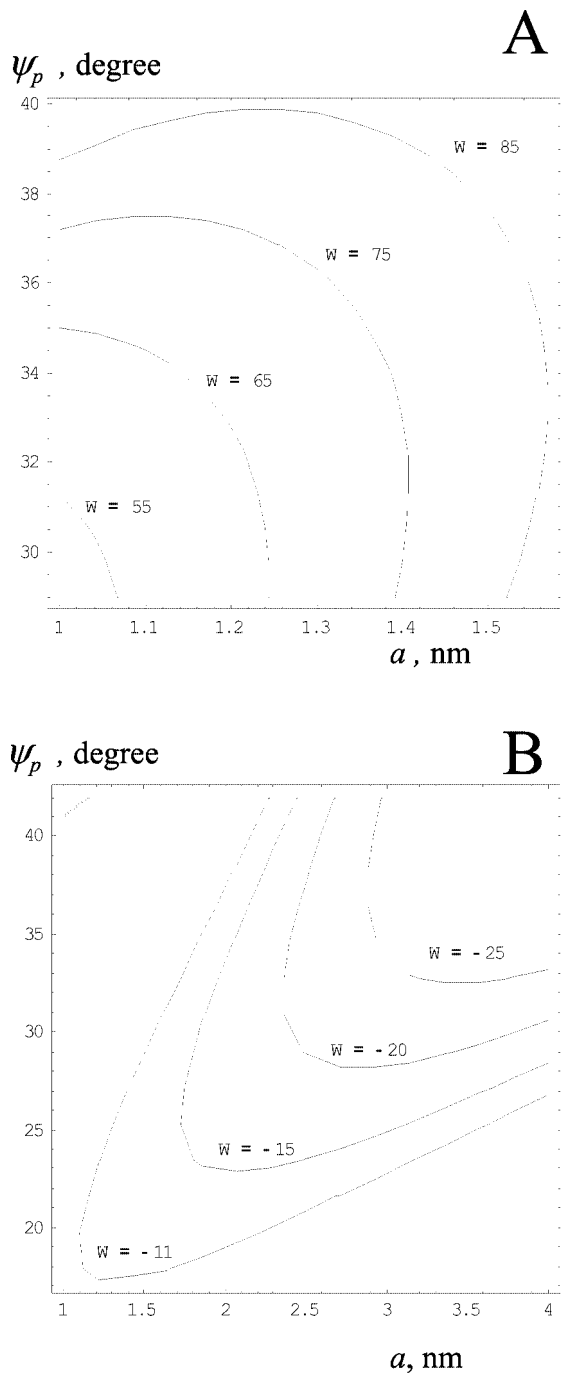

FIGURE 7 Isergones, lines of equal free energy at the plane with coordinates stalk radius a_s-peel-off angle ψ_p. Effective hydrophobic surface tension $\gamma_{eff} = 0.48\ k_BT/nm^2$. (*A*) $c_0 = 0$. (*B*) $c_0 = -0.348\ nm^{-1}$.

$-0.1\ nm^{-1}$. Both curves display a minimum. However, positions of these two minima are quite different. The bilayer with no spontaneous curvature has a minimum of 50 kT at $\psi_p = 26.4°$, whereas in the second case there is much lower minimum of 28.8 kT at $\psi_p = 22.2°$.

When the stalk enlarges, the energy of hemifusion as well as the peel-off angle change. Fig. 7 presents the free energy of hemifusion as a function of stalk radius a_s and peel-off angle ψ_p for different spontaneous curvatures of monolayers. Effective hydrophobic surface tension was assumed equal to $\gamma_{eff} = 0.48\ k_BT/nm^2$. The lines connect the points with equal free energy of the system, and following the tradition of using Greek names for such types of curves (e.g., isochors and isobars), we shall call them isergons. (The term was proposed by A. J. Hudspeth.)

As one can see here the energy of the hemifusion structure quickly increases with its radius unless spontaneous curvature is very high as in Fig. 7 *B* where we took dioleoylphosphatidylethanolamine (DOPE) spontaneous curvature $c_0 = -0.348\ nm^{-1}$. This is somewhat puzzling because this would virtually preclude the initial hemifusion structure from evolving into transmembrane contact as in Fig. 1 *C* and would be even less favorable for an extended trilaminar structure.

However, there is a possibility that the actual void hydrophobic energy can be drastically decreased. The void energy can be very large for pure bilayers of a single lipid component, but it will significantly decrease for bilayers formed from lipid mixtures or containing small amount of impurities, which may fill the voids. Siegel (1999) noted that in biological membranes, the voids forming around the stalk might have much lower energy because they could be filled up with some impurities always present in the membrane. Even minute fractions of apolar lipid like triglycerides and dolichol could lower the energy of TMCs by up to 50 to 80 kT. This might practically eliminate the hydrophobic energy of interstices, reducing the total energy of intermediate structures to the bending energy only.

But is there enough oil in the membrane to fill the hemifusion interstices? The equilibrium solubility of long chain alkanes or other long chain apolar oils in a bilayer is typically a few volume percent. For our estimate let us take the lower limit of 1% only. Then for the initial hemifusion structure with $a_s = 1$ nm, the necessary amount of oil would be found in two fusion bilayers inside the circle with radius of 3.13 nm. This hardly exceeds the bent portion of the bilayers involved in hemifusion. Therefore, enough oil can be squeezed just from the stalk proper to fill up the interstices. This result holds for a moderate enlargement of the hemifusion so that the hydrophobic void energy can be drastically decreased if not eliminated completely. To illustrate this we repeated the previous calculation for effective surface tension reduced to 1/5 of its tentative value and $c_0 = -0.1\ nm^{-1}$. Then the initial hemifusion structure has less than 5 kT of energy; when the radius a_s increases from 1 to 2 nm, the energy grows only to 10 kT. In this case all the evolutions leading to stalk enlargement, to transmembrane contact, and to complete fusion become eminently possible.

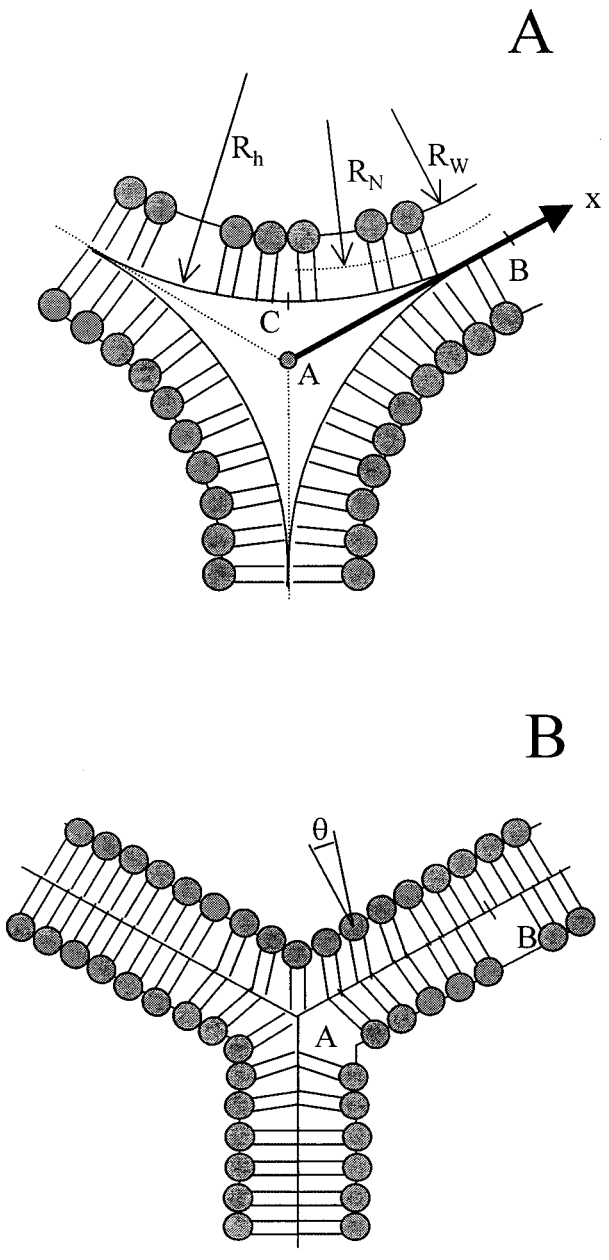

FIGURE 8 Tilt deformation in H_{II} phase. (*A*) Cross-section of the void space between three lipid cylinders. (*B*) Collapse of the void space.

Deformation of tilt

Another way to eliminate the voids in the hemifusion structure is to shift lipid molecules to the void space. In principle, lipid molecules can displace in the direction normal to the monolayer, and by doing so they could fill up the voids of hemifusion (Fig. 8). Of course this would happen at a cost. Normal displacement of lipid molecules represents a different kind of membrane deformation—deformation of tilt. During the last decade, the deformation of tilt attracted the attention of many researchers (Mackintosh and Lubensky, 1991; May, 2000; Hamm and Kozlov, 2000 and references therein). Kuzmin et al. (2001) suggested that this deformation can occur during membrane fusion and hence should be taken into consideration. Let us estimate the energy cost that could be expected for this deformation and if it will be compensated by the release of hydrophobic energy after void collapse.

As a specific example let us consider the interstices in the H_{II} phase (Fig. 8 *A*) formed by DOPE (Siegel, 1993; Fuller and Rand, 2001). Assuming that the lipidic phase has the shape of circular cylinders Siegel called the hydrophobic voids between them trilaterally symmetric voids. In cross section (Fig. 8 *A*) these voids have the shape of curvilinear triangles. Siegel estimated the energy required to produce a unit length of such void configuration equal to 41.6 pN or 5 kT/nm.

Is it possible that the void space between three H_{II} cylinders would collapse, i.e., that the three monolayers in Fig. 8 *A* deform in such a way that they would fill up this void space? To answer this question one has to compare the energy of the void W_{TV} including the hydrophobic energy of the tails and bending energy of initial monolayers with deformation energy of the collapsed void $W_{collapse}$. The system will acquire configurations with lower energy.

Deformation of tilt can be described by parameter of tilt that in a simple case can be visualized as an angle θ between the axis of lipid molecule and the normal to the monolayer. Departure of this angle from 0° exposes a portion of hydrophobic surfaces of lipid molecules and hence increases the energy of the monolayer. To take this into consideration one has to add to the bending energy (Eq. 1) an additional term with tilt energy $\frac{1}{2}\kappa_\theta\theta^2$. In line with Eq. 1, one can also include into this expression a certain spontaneous value of tilt θ_0, changing it to $\frac{1}{2}\kappa_\theta(\theta - \theta_0)^2$. However, here we limit ourselves to the simplest form of the tilt energy.

Collapse of the void in Fig. 8 means that the upper monolayer CB shifts to position AB and becomes planar. The other monolayers lining the void are transformed in a similar way. The orientation of lipid molecules—tilt angle $\theta(x)$—in the new, planar configuration of the monolayer between A and B changes from $\pi/6$ to 0:

$$\theta_A = \frac{\pi}{6} \quad \text{and} \quad \theta_B = 0. \tag{33}$$

Let us find the deformation energy of planar monolayers in the collapsed configuration. At first glance it might seem counterintuitive but the planar monolayer AB has not only tilting but also bending energy. This statement deserves some additional explanation although it was already presented in Hamm and Kozlov (2000) and Kuzmin et al. (2001).

What is the nature of the bending deformation? It is actually the change of the shape of lipid molecules.

Bending results in different changes of the cross section (not simply the size) of heads and tails of lipid molecules. The curvature of the initial monolayer CB is negative so that lipid heads are compressed and tails are expanded. Axes of lipid molecules have different orientation in space, although they remain normal to the monolayer surface: there is no tilt. Now let as perform a gedanken experiment: transform monolayer CB into monolayer AB in such a way that all orientations of lipid molecules are preserved. In this transformation the lipid molecules slide along each other (along their axis) without changing their molecular shapes. Therefore, the bending energy determined by the shape of the molecules is preserved. Now from comparison of molecular orientation of the monolayers CB and AB it is not difficult to figure out that in the new, planar configuration AB the role of curvature c is played by the derivative $d\theta/dx$. Transition from CB to AC involves a certain work due to exposure of lateral surfaces of lipid molecules to aqueous surrounding, which is proportional to θ^2. The density of deformation energy in the collapsed monolayers can be presented as

$$w_{\text{def}}(x) = \frac{1}{2}\,\kappa\left(\frac{d\theta}{dx} - c_0\right)^2 + \frac{1}{2}\,\kappa_\theta\theta^2 \tag{34}$$

Here, as before, κ is the bending modulus, whereas κ_θ is the tilt modulus.

The total deformation energy of the collapsed void per unit length is

$$W_{\text{collapse}} = 6\int_{\text{A}}^{\text{B}} w_{\text{def}}(x)dx, \tag{35}$$

where coefficient 6 accounts for six equivalent parts of the total perimeter of the void cross section.

Of course orientation of lipid molecules in the planar monolayer AB will not remain the same as in the original monolayer CB. It will relax to the new positions $\theta(x)$ to minimize the energy of the total monolayer. According to calculus of variations, the function $\theta(x)$ that minimizes the integral (Eq. 35) is determined by the Euler equation

$$\kappa\,\frac{d^2\theta}{dx^2} - \kappa_\theta\theta = 0 \tag{36}$$

As one can see from the dimension analysis, this equation defines a characteristic constant of length,

$$\tau = \sqrt{\frac{\kappa}{\kappa_\theta}}, \tag{37}$$

that gives the range of the monolayer where tilting and bending of lipid molecules occur. Beyond this range the planar monolayer is free of both tilting and bending. Notice that spontaneous curvature c_0 that was present in the deformation energy Eq. (34) disappeared from the Euler Eq. 36. Boundary conditions for this differential equation are given by Eq. 33.

Solution of the Euler Eq. 36 is

$$\theta(x) = \frac{\theta_{\text{A}}\,\sinh[(l-x)/\tau]}{\sinh[l/\tau]} \tag{38}$$

in which l is the distance between points A and B and deformation energy is

$$W_{\text{collapse}} = 6\left\{\frac{1}{2}\,\theta_{\text{A}}^2\sqrt{\kappa\kappa_\theta}\,\coth\frac{l}{\tau} + \kappa c_0\theta_{\text{A}} + \frac{1}{2}\,\kappa c_0^2 l\right\} \tag{39}$$

To estimate the collapse energy W_{collapse} one needs to know the value of the tilt modulus κ_θ. Unfortunately there are no direct experimental measurements of this material constant. In the absence of direct measurements Hamm and Kozlov (2000) estimated it at 40 mN/m, whereas Kuzmin et al. (2001) came up with 33 mN/m. Although these estimates were based on different models, the results are rather close and can be summarized as 9 kT/nm^2. That gives the characteristic length $\tau = 1.05$ nm.

The other parameters can be taken from Fuller and Rand (2001): $R_{\text{h}} = 4$ nm, $R_{\text{N}} = 2.9$ nm, $R_{\text{W}} = 2.18$ nm, $\lambda = 0.73$ nm, and $c_0 = -1/R_{\text{N}}$. Then the energy of collapsed void is 4.1 kT/nm. This result is not very different from the open void energy of 5 kT/nm found by Siegel (1999); therefore, these two configurations are energetically virtually equivalent.

Equation 39 can be used for estimation of the energy of the trilaminar structure that could appear after further expansion of the stalk. Using the fact that the open void has approximately the same energy as the collapsed one, we shall use this equation for our estimation. Notice that the last term in Eq. 39 represents the energy of the monolayer in the initial, planar state. If we refer the energy of the trilaminar structure to the planar state, then this amount should be subtracted from the final energy. Besides, we assume that the length l is large in the characteristic scale of the system, i.e., it considerably exceeds 1 nm. Then the energy of the unit of length of the trilaminar contact is given by

$$f_{\text{tri}} = 6\{\tfrac{1}{2}\,\theta_{\text{A}}^2\sqrt{\kappa\kappa_\theta} + \kappa c_0\theta_{\text{A}}\} \tag{40}$$

The physical meaning of this quantity is a linear tension, which is why the designation f is used here.

To estimate the linear tension of the trilaminar contact, consider bilayers without spontaneous curvature. Then $f_{\text{tri}} = 7.8$ kT/nm. The presence of negative spontaneous curvature noticeably decreases this tension; for example, if $c_0 = -0.1$ nm^{-1} then $f_{\text{tri}} = 4.7$ kT/nm. This linear tension can even become zero, if $c_0 = -(\theta_{\text{A}}/2)\sqrt{\kappa_\theta\kappa} = -\theta_{\text{A}}/2\tau$. Numerically it gives $c_0 = -0.25$ nm^{-1}, which is not very far from the spontaneous curvature of DOPE that readily forms the H_{II} phase.

In the absence of spontaneous curvature there is only one term, $\frac{1}{2}\,\theta_A^2\sqrt{\kappa\kappa_\theta}$, left in the braces of Eq. 40. This term represents both bending and tilting energy, which give equal contributions to the total trilaminar energy. This can be demonstrated in the following way. Angle θ exponentially decreases with coordinate: $\theta(x)=\theta_A \exp(-x/\tau)$. Therefore, the tilting energy changes as $w_{tilt}(x)=(\kappa_\theta\theta_A^2/2)\exp(-2x/\tau)$. After integration it becomes $\frac{1}{4}\,\kappa_\theta\tau\theta_A^2 = \frac{1}{4}\sqrt{\kappa\kappa_\theta}$. This is exactly one-half of the total energy of thetrilaminar structure. The other one-half is contributed by the bending energy.

Complete fusion-fusion pore

The next step after formation of the hemifusion structure is rupture of the *trans* monolayers and completion of the fusion process (Fig. 1 *D*). At this moment a fusion pore is formed, and the fusion process is completed. Here we analyze the energetic cost of the fusion pore and of its consequent enlargement. In the previous sections we have considered the free energy associated with bilayer wings included in the hemifusion structure. It was found that its energy contribution was insignificant. However, this does not mean that completely fused bilayers have negligible energy. The reason is that the bending energy is concentrated at the neck of the fusion pore.

In the literature there are different approaches to the calculation of this energy. In the simplest one (Markin et al., 1984; Chizmadzhev et al., 1995) the bilayer is visualized as a single layer with bending rigidity equal to the sum of the bending rigidity of the monolayers. Originally this model was called a bilayer stalk and it resulted in the same equations that were derived from a monolayer stalk. In the old model the minimal energy of such a bilayer stalk with bending rigidity 10^{-19} J was found to be 90 kT (Chizmadzhev et al., 1995). However, this is a gross underestimation because two monolayers are bent quite independently, and their elastic energy should be calculated separately. If this were done, then this value would increase to 150 kT.

So the old model predicts very high elastic energy for a fusion pore due to the assumption of a circular shape for its neutral surface. In the present approach the shape of the neutral surface is calculated with constant total curvature. As we have seen above, for a single monolayer this results in the stress-free stalk. However, this result cannot be extended to a bilayer because its monolayers cannot be made stress free simultaneously. However, their energy can be made much lower than in the old model.

We calculate the bending energy of the bilayer using the equations derived in the Hemifusion section. We select the interface between two monolayers as a reference surface (Fig. 1 *D*). Its principal curvatures c_m and c_p are defined the same way as for a monolayer stalk by Eq. 5. The principal

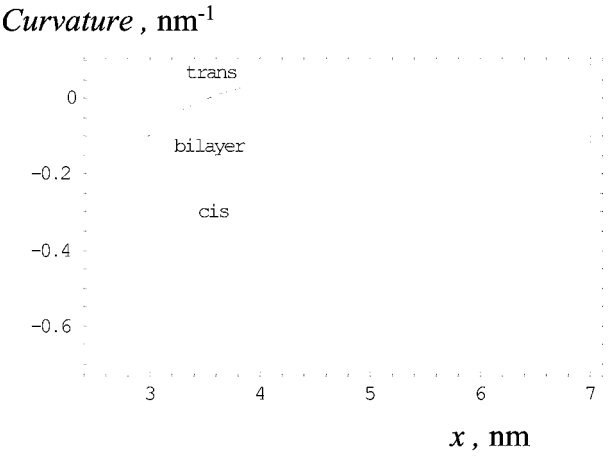

FIGURE 9 Curvature of *cis* and *trans* monolayers in a bilayer lining out a minimal fusion pore with radius of 0.5 nm. The bilayer has constant geometrical curvature c^b equal to -0.01 nm^{-1}.

curvatures of the *cis* and *trans* monolayer are defined at their respective neutral surfaces and are presented by Eqs. 21 and 22. As we mentioned before these definitions are consistent for both monolayers: if the monolayer in a given principal plane is convex, then the given curvature is positive and vice versa. However, two monolayers are bent in the opposite directions. For an example, let us consider parallel curvatures at the equatorial plane. According to our convention, the bilayer parallel curvature c_p here is positive, and the radius of the bilayer parallel curvature obviously exceeds the monolayer thickness: $R_p = 1/c_p > h$. From Eqs. 21 and 22 one finds that $c_p^{cis} > 0$ and $c_p^{trans} < 0$, just confirming that two monolayers are bent in the opposite directions and determining the sign of their curvature.

Now let us see how the curvature of both monolayers varies along the bilayer. We shall look for the solution where the reference surface of the bilayer has a constant total curvature $c_m + c_p = c^b$ and the radius of its "waist" is a_b. Then the principle curvatures of the bilayer are

$$c_p = \frac{1}{2}\,c^b + \frac{a_b}{x^2}\left(1 - \frac{1}{2}\,a_b c^b\right)$$

and

$$c_m = \frac{1}{2}\,c^b - \frac{a_b}{x^2}\left(1 - \frac{1}{2}\,a_b c^b\right) \qquad (41)$$

These equations are similar to the stalk equations, but here it is explicitly stressed that the radius of the bilayer waist is a_b. As one can see, the sum of these two curvatures (total curvature, $c_{tot} = c_p + c_m$) equals c^b, but for separate monolayers this sum is not a constant but rather varies along the bilayer. Fig. 9 illustrates how the total curvature of *trans* and *cis* monolayers varies with x for different values c^b equal correspondingly to -0.1, -0.01, and -0.001 nm^{-1}.

A horizontal line in each panel presents the total curvature of the bilayer reference surface.

It is important to note that close to the neck (at small x) the total curvature of both monolayers has the same sign and it is negative. At first glance this might seem counterintuitive because two monolayers are oriented in the opposite directions. If the bilayer had the form of a sphere, then the outer monolayer would have positive total curvature, whereas the inner monolayer would have negative. However, around the pore two fused bilayers have a saddle-type shape with rather subtle interplay between parallel and meridianal curvature. As one can easily see, at the *cis* monolayer the meridianal curvature plays the dominant role and it is negative. That is why the total curvature of the *cis* monolayer is negative. The situation is reversed at the *trans* monolayer: here the dominant role is played by parallel curvature and it is negative. So the total curvature of the *trans* monolayer is also negative. At a farther distance the total *trans* monolayer curvature changes sign, whereas the *cis* monolayer curvature remains always negative.

If the bilayer curvature is high (Fig. 9), the difference between two monolayer curvatures is rather pronounced. If the absolute value of the bilayer curvature decreases, the difference between two monolayers gradually disappears and the two curves approach each other.

Other parameters of the bilayer can be found from Eqs. 24 through 27 by substituting $x_p = a_b$ and $\sin \psi_p = 1$. The bending energy of the bilayer is given by the integral (Eq. 27) over the total area of the reference surface from $x = a_b$ to b_b. The energy depends on the constant curvature of the bilayer c^b, on the radius of the neck a_b, on the spontaneous curvature of two monolayers c_0^{cis} and c_0^{trans}, and on the position of neutral surface of each monolayer. For the sake of comparison with previous results the neutral surface is taken in the middle of each monolayer, i.e., $\lambda = h/2$, the monolayer thickness h is 2 nm, and the monolayer bending rigidity κ is 10 kT.

The results of calculation are presented in Fig. 10. The curvature of the bilayer reference surface c^b is assumed negligibly small. Fig. 10 *A* presents the energy of a symmetric bilayer comprised of monolayers with equal spontaneous curvatures: $c_0^{cis} = c_0^{trans}$. As one can see, the bigger the radius of the neck a_b, the smaller the bending energy of the bilayer. We presented these curves in the range of a_b beginning from $a_b = 2.5$ nm because the radius of the fusion pore hardly can be smaller than 0.5 nm (Kuzmin et al., 2001). At this radius the bending energy reaches its highest value. If the monolayers have zero spontaneous curvature the bending energy amounts to 50 kT. This is a drastic decrease from the old model estimate of almost 150 kT (Chizmadzhev et al., 1995). However, this barrier quickly decreases if the monolayers have even a small negative spontaneous curvature. At the very modest spontaneous curvature of -0.05 nm^{-1} the energy starts from approximately 25 kT, and already at the pore radius of 1.5 nm it becomes negative. If spontaneous curvature is more pronounced and reaches -0.1 nm^{-1}, the bending energy is negative from the very beginning and it decreases with the growing radius.

It would be rather instructive to dissect the curves in Fig. 10 *A* splitting them into two components contributed by *cis* and *trans* monolayers. This is done in Fig. 10 *B* and *C* for spontaneous curvatures 0 and -0.1 nm. In the absence of spontaneous curvature (Fig. 10 *B*), *cis* and *trans* monolayers store about the same bending energy so that the total energy of the bilayer is simply the double monolayer energy. However, if two monolayers have negative spontaneous curvature (Fig. 10 *C*) they behave quite differently. The *trans* monolayer stores positive energy, which, after a shallow minimum, grows with neck radius. Therefore, the *trans* monolayer with negative spontaneous curvature does not like to be bent into a fusion pore. However, the *cis* monolayer has negative energy that more than compensates the *trans* monolayer, so that the total energy of the bilayer is negative and it decreases with neck radius. Even better results can be obtained with an asymmetric bilayer.

Now let us consider how bending energy is distributed along the bilayer. One can anticipate that it is mainly concentrated in the neck of the fused bilayers rather than in its "wings." Let us select an arbitrary point with coordinate x_w and find the energy stored beyond this point, $x > x_w$. It means that the integral (Eq. 27) should be taken over $x > x_w$. The results show that the energy stored in the "wings" quickly decreases with x_w and at the distance of only 1 nm the wings carry only 5% of the total energy. That means that in more complicated cases of hemifusion presented in Fig. 1, *B* and *C* one should be concerned mainly with the neck of the intermediate structure.

Position of the neutral surface

In the previous calculation we placed the neutral surfaces of monolayers exactly in their middle. However, the neutral surface is believed to be shifted in the direction of polar heads so that $\lambda < h/2$. This position is not very well known and only a few direct measurements are published. Recently Fuller and Rand (2001) performed a detailed study of the geometrical and elastic properties of hexagonal-forming lipid, DOPE, and the influence of lysolipids on these properties. Position λ was estimated between 0.69 and 0.77 nm with mean value of 0.73 nm. In the absence of direct measurements of λ for bilayer forming lipids we shall consider the distance λ between this value and the position in the middle of the monolayer. Fig. 11 shows how the energy of two fused bilayers would change with different position of neutral surface. The free energy of the fusion pore W_{fp} is presented as a function of pore radius r_p for $\lambda = 1.0$ and 0.73 nm and a few selected values of spontaneous curvature. The general tendency is the increase of W_{fp} with decreasing λ. If

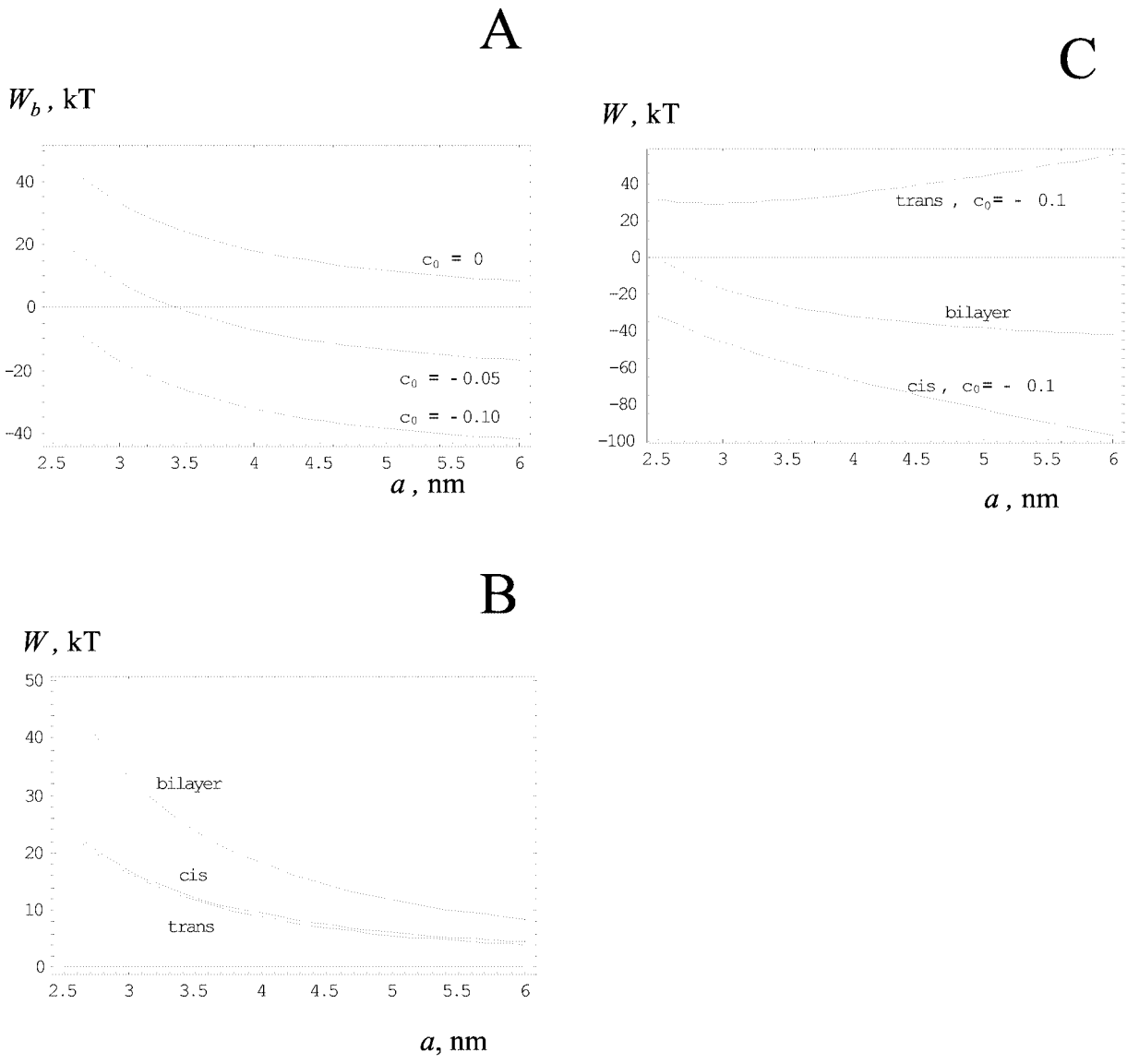

FIGURE 10 Bending energy of bilayers and individual monolayers as the function of the neck radius a_b. Bilayers have constant geometrical curvature close to zero and the distance λ from the hydrophilic surface of the bilayer to the neutral surface is taken equal to $h/2 = 1$ nm. (*A*) Three symmetric bilayers with monolayers having spontaneous curvature equal to 0.0, -0.05, and -0.1 nm^{-1}. (*B*) Symmetric bilayer comprised of monolayers with no spontaneous curvature. (*C*) Symmetric bilayer with monolayers having $c_0 = -0.1$ nm.

the monolayers have no spontaneous curvature, the initial energy of the fusion pore changes from 50 to 87 kT. However, if the monolayers have some spontaneous curvature, the increase of spontaneous energy is not very significant. For example, if $c_0 = -0.1$ nm^{-1} then the energy changes from -1 to $+24$ kT. These are quite modest energies and, in addition, they quickly decrease with increasing pore radius.

From hemifusion to complete fusion

Having calculated the energy of hemifusion structures and completely fused bilayers with the fusion pore we are now in a position to determine the possible path of transition between them. Fig. 12 presents the energy landscape of these two states with coordinates a_s, peel-off angle ψ_p, and free energy W. Spontaneous curvature was assigned a very modest value of -0.05 nm^{-1} and surface tension in the interstices $\gamma_{eff} = 0.096$ mN/m. The line denotes the path of fastest descent. One can see that if the hemifusion starts at the minimum stalk radius $a_s = 1$ nm, then the minimum hemifusion energy of 12.9 kT corresponds to a peel-off angle of 14.5°. Then this line climbs to the pass at the level $W = 46.5$ kT and $\psi_p = 26.6°$. At this level the hemifusion energy and complete fusion energy become equal, and one can expect transition to complete fusion. After this the

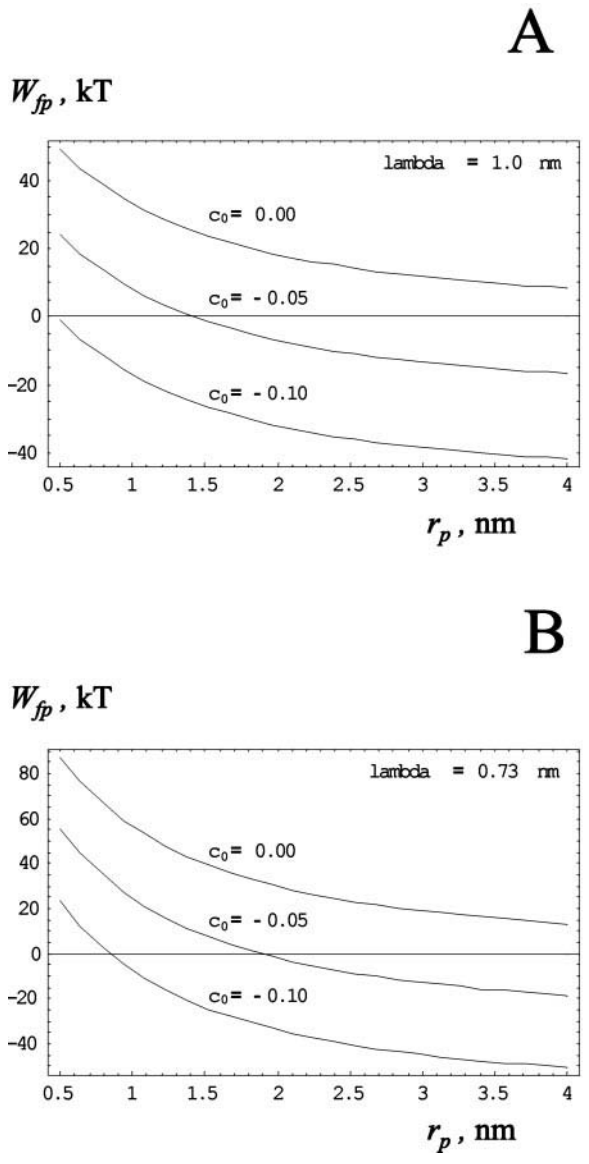

FIGURE 11 Dependence of the energy of the fusion pore on pore radius r_p for a few selected values of spontaneous curvature indicated in the picture. (*A*) $\lambda = 1.0$ nm; (*B*) $\lambda = 0.73$ nm.

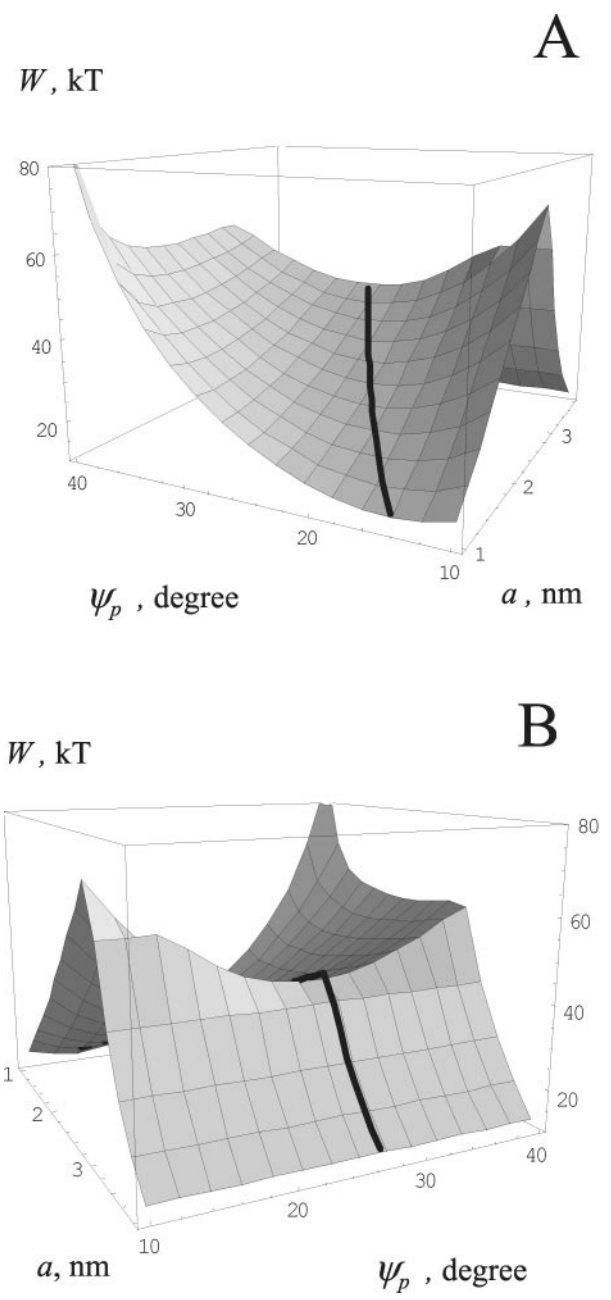

FIGURE 12 Energy landscape of transition from hemifusion to complete fusion and the path of fusion; the line shows the path of steepest descent or the path of fusion; $c_0 = -0.05$ nm^{-1}, $\gamma_{eff} = 0.096$ mN/m. (*A*) View from the side of hemifusion. (*B*) View from the side of complete fusion.

transition path steeply drops so that the fusion pore enlarges and fusion is complete.

DISCUSSION

We presented here a corrected version of the membrane fusion mechanism that we call the stress-free stalk model. Since its introduction and consequent mathematical analysis (Hui et al., 1981; Kozlov and Markin, 1983; Markin et al., 1984) the original stalk model was accepted as a universal type of lipidic intermediate in biological and model membrane fusion. The stalk emerges after initial membrane perturbation as a result of merging of proximal or *cis* monolayers and it provides an hour-glass shaped connection between the membranes. When one looks at the drawing of the stalk (Fig. 1), it becomes immediately evident that the monolayer in the stalk is strongly bent. However, inertia of two-dimensional visualization often makes people assume that the bending has a negative sign. In a recent issue of *Biophysical Journal* one can read the following statement: "The stalk structure is a highly negatively curved connection between opposing monolayers that leads to hemifu-

sion" (Fuller and Rand, 2001). While it is true that membrane is strongly curved in a stalk, it is not correct to conclude that the curvature is highly negative. The monolayer in the stalk is saddle-shaped (Fig. 2 *B*) such that two opposite curvatures can completely compensate each other. So the total curvature of the stalk can be very small, although negative. If the *cis* monolayer has a certain negative spontaneous curvature, then the stalk can adjust its shape to accommodate this curvature and the resulting structure can become completely stress free, thus not accumulating any elastic energy (apart from Gaussian curvature). If the initial, reference state of this monolayer was planar, then the frustration energy is released and the energy of the stalk, defined as the difference between final and initial state, becomes negative, in contrast to the common belief that the stalk should carry rather high positive bending energy.

We calculated the shape of the stress-free stalk and determined its geometrical and energetic characteristics. This is the main result of the mechanical analysis performed in this paper. It is important to note that there are no adjustable or postulated parameters in the stress-free stalk model: all characteristics were calculated and found from basic physical principles. The energy of the stalk was found to be much lower than in the original model (Kozlov and Markin, 1983) where the stalk was postulated to have a circular shape. Unfortunately, this erroneous original assumption of the circular shape was adopted in numerous subsequent papers devoted to the stalk model. Needless to say, these results should also be reconsidered. Credit must be given to D. Siegel who, although using the assumption of the circular shape of the stalk, felt that something was troubling about it. He wrote: "the geometric model used for some surfaces of stalk and TMCs (circular toroids) may be a gross simplification. This implies that the corresponding surfaces in real intermediates would deform into different shapes with lower free energy" (Siegel, 1999). We believe that the stress-free stalk model solves this problem and removes the unjustified simplification. Obviously, this model should be used in future attempts to define the path of evolution of the total process of membrane fusion.

We applied the stress-free stalk model to an analysis of hemifusion and consequent transition to complete fusion. We found that the energy barriers, which in previous approaches looked insurmountable, now became quite moderate and could be reasonably overcome.

One of the energetic obstacles to membrane fusion is represented by the void interstices that form at the neck of the stalk (Fig. 1 *B* and Fig. 6). The problem of voids is rather controversial and it is not completely resolved at the present time. D. Siegel, who pointed out the existence of this feature in the mechanism of fusion, proposed a possible solution (Siegel, 1999): impurities that are always present in the membranes can fill these interstices and drastically reduce their hydrophobic energy.

In this context we note the paper by Basanetz et al. (1998) aimed at determining if hydrocarbons or other nonpolar lipids could facilitate phospholipase C-promoted fusion of large unilamellar vesicles. These authors found that low proportions (up to 5 mol%) of single-chain lipids promoted fusion and that small amounts of hexadecane or squalene significantly enhance fusion rates in their system. These observations were interpreted to result from decreased interstitial energy of the stalk connecting the two apposed bilayers.

Based on Siegel's proposal we considered reduced hydrophobic energy of interstices and analyzed the possible evolution of a stalk from hemifusion to complete fusion. The transformation of intermediate fusion structures can be characterized by three parameters: the radius of the stalk, the peel-off angle at the interstices, and the energy of the system. In this three-dimensional space we have calculated the energy landscape corresponding to these intermediates (Fig. 12). The evolution of the system proceeds along the line of steepest descent in this hilly landscape, goes over the pass on the energy "ridge," and then steeply drops to the final state of complete fusion. This qualitative picture should be rather universal, whereas the numerical characteristics of this process should depend on specific properties of fusing membranes. To get a feeling for possible numbers we considered here one particular example with very modest spontaneous curvature of $-0.05\ \mathrm{nm}^{-1}$ and $\gamma_{\mathrm{eff}} = 0.096$ mN m^{-1} presented in Fig. 12. The initial membranes are assumed to be in a planar state, which is taken as a reference. Formation of the stalk and emergence of the initial hemifusion structure (Fig. 1 *B*) is accompanied by an increase of free energy to approximately 13 kT (Fig. 12). To complete the fusion the system should climb up the slope to the point at the energy ridge with the "altitude" of 46 kT, corresponding to a stalk radius of 3.13 nm. Recall that this radius is the distance from the axis of revolution to the neutral surface of the stalk monolayer (Fig. 1 *A*). If the transition to the fusion pore occurred here then the radius of the fusion pore lumen would be 0.13 nm and then it would expand.

If parameters of the fusing bilayers were different, then the characteristics of the fusion path would change. The barriers are rather sensitive to these changes and could increase (or decrease) considerably. However, the radius of the stalk corresponding to the transition of hemifusion to the fusion pore would change very little so that we could safely say that the radius of the initial fusion pore would be in the range 0.1 to 0.5 nm in accordance with general expectations.

It is interesting to compare these numbers with experimental data for barriers in membrane fusion. For example, in the fusion of secretory granules with mouse mast cell plasma membrane, Oberhauser et al. (1992) reported the activation energy of fusion pore formation of 23 kcal/mol = 38.9 kT. For the pH-induced fusion between vesicular stomatitis virus and erythrocytes ghosts (Clague et al., 1990)

the activation energy of lipid mixing was found to be 42 kcal/mol = 71 kT.

Lee and Lentz (1998) studied the onset of polyethylene glycol-mediated vesicular fusion by monitoring lipid mixing and the transfer of protons between two vesicles. They measured the activation energy E_{act} of the individual steps of fusion and found three barriers in this process that were interpreted as the stalk formation barrier, the hemifusion, and fusion pore formation. The stalk formation had an activation energy $E_{act}^{stalk} = 37$ kcal/mol = 62.5 kT, hemifusion had $E_{act}^{hemi} = 27$ kcal/mol = 45.6 kT, and fusion pore formation had $E_{act}^{pore} = 22$ kcal/mol = 37.2 kT.

It is known that there are significant difficulties in interpreting activation energy data. However, all these numbers are close enough and they indicate that the theoretical estimates provided above probably caught essential features of the fusion process. Besides this, there is another point that should be made here. From the striking similarity of activation energy in different systems, Lee and Lentz concluded that the basic molecular processes occurring in secretory and viral fusion involve a set of lipid molecule rearrangements that are also involved in model membrane fusion.

Another point to discuss is the proper selection of the neutral surface in the fusion monolayers. In the early models it was localized to the middle of the monolayer. How is this issue addressed in the stress-free stalk model? For the stalk per se this question is immaterial: we have calculated the shape of the neutral surface itself, therefore the result is correct wherever in the monolayer it is located. It is also not important for hemifusion for the following reason: the hemifusion structure (Fig. 1 *B*) consists of the stalk, the dimples, and the bilayer wings. The dimples, as well as the stalk, were described by their neutral surfaces covering a spherical sector with a certain body angle. Only the body angle determines the bending energy of a spherical segment formed by a monolayer. Hence, it also does not matter where this surface is located.

The rest of the hemifusion structure is formed by the bilayer. The bilayer bending energy depends on the position of the neutral surface. However, the wings in the hemifused state carry a very small portion of the energy of the hemifusion structure. Therefore, the error in its estimate does not noticeably change the total energy. This question can be relatively important for the calculation of the fusion pore energy as was demonstrated in the corresponding section. When the neutral surface is shifted closer to the lipid heads the energy of the fusion pore increases. In the analysis of transition from hemifusion to the fusion pore it will lead to some increase of the barrier and increase of the initial pore size. As we mentioned above the size of the pore can vary between 0.1 and 0.5 nm. The increase of the barrier by a few dozens percent is quite possible and, indeed, might even better correspond to experimental observations.

Let us return to the question of the hydrophobic interstices. As was suggested by D. Siegel, they can be filled up by the impurities present in the membrane. However there is another way to achieve the same goal: to deform the monolayer in the normal direction. In this case a sharp point—a beak—would appear at the contour. In previous models such deformations were ignored and only smooth curves were allowed. The shift of lipid molecules in the normal direction represents the deformation of tilt that in the last decade has attracted attention of researchers. There might be a possibility that by allowing such deformation the filling of the gaps could be achieved at a lesser energy cost than preserving the hydrophobic voids. We calculated the energy of the hypothetical tilt deformation at the H_{II} phase of DOPE and found that it is about equal to the energy previously estimated for the hydrophobic voids. Therefore in this case the tilt deformation does not provide any energy gain. This does not mean that tilt deformation could not occur in the H_{II} phase. On the contrary, the equality of these two energies indicates that both conformations are possible and that they should exist simultaneously in the H_{II} phase. This means that in the hemifusion structure the tilt deformation would not provide significant decrease of energy, and filling the interstices with impurities is the much more beneficial solution of the problem. In this context it is probably best to avoid using the term "impurities" for some minor components that are always present in biological, and even in model membranes, and can play such an important role in membrane physiology.

Based on the fact that hydrophobic void and interstices with tilt deformation have similar energies we calculated the linear tension of the trilaminar contact or the perimeter on the trilaminar structure. This has a rather high value of 7.8 kT nm^{-1} that seems to prohibit formation of any extensive trilaminar diaphragm. In a recent review Stegmann (2000) underlined that the hemifusion diaphragm was estimated to be no wider than 1 nm. The same reasoning caused Frolov et al. (2000) to avoid describing the actual geometrical structure of the hemifusion diaphragm and instead guardedly phrase its definition as follows: "Operational definition of the term 'hemifusion' is the state of two interacting bilayers where the mixing of lipidic components occurs without the mixing of aqueous contents." It is true that the existence of linear tension at the perimeter of the trilaminar diaphragm forces it to collapse. However, it only means that small diaphragms cannot exist. The larger trilaminar diaphragm can be rescued by membrane tension. If the fusing bilayers have membrane tension γ_b and the trilaminar diaphragm has a circular shape of radius r_{tri} then the equilibrium between them can be described by a two-dimensional analog of the Laplace equation (Volkov

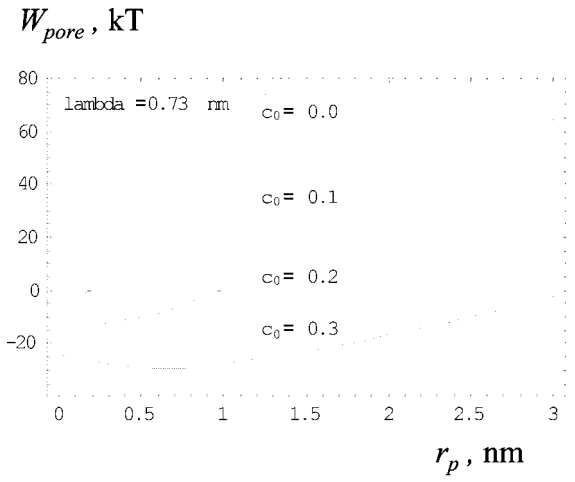

FIGURE 13 Bending energy of the pore edge, $r_p = a - \lambda$, $\lambda = 0.73$ nm.

et al., 1998) and the critical radius of the diaphragm can be found as

$$r_{tri} = \frac{f_{tri}}{2\gamma_b} \tag{42}$$

The trilaminar structure can exist if its radius exceeds this value. The bilayer tension is usually of the order of $\gamma = 2$ mN m^{-1} = 0.48 kT nm^{-2}. The linear tension of the trilaminar contact was estimated above as $f_{tri} = 7.8$ kT m^{-1} for $c_0 = 0$, and 4.7 kT m^{-1} for $c_0 = -0.1$ nm^{-1}. The critical radius of the trilaminar structure for these two cases is 8.1 and 4.9 nm, correspondingly. Therefore small trilaminar structures should either close up or overcome the barrier at the critical radius and then reach a certain equilibrium size. There is no physical reason why an extended trilaminar structure could not exist.

The new stress-free stalk model has an important bearing on the analysis of hydrophilic pores in a single lipid bilayer (Chernomordik et al., 1987; Neumann and Kakorin, 2000; Melikov et al., 2001). The pore edge is similar to the stalk with the inverted monolayer and hence with opposite sign of the curvature. However there is one important difference: the thickness of the bilayer, which is equivalent to the height of the stalk, is constant. Taking this into consideration we calculated the energy of the pore as a function of its radius for a few selected spontaneous curvatures of the monolayers (Fig. 13). The new model predicts much lower pore energy. With increasing spontaneous curvature the pore energy decreases. The curve for zero spontaneous curvature starts slightly above zero energy and increases with pore radius. Interestingly, at $c_0 = 0.1$ nm^{-1} the initial pore energy is negative but with increasing radius it becomes positive. However, if spontaneous curvature is increased to 0.3 nm^{-1} the curve remains negative throughout the long range of radii up to 2.5 nm. It also displays a minimum at $r_p = 0.5$ nm although a shallow one. So the new model gives much smaller pore energies than the previous one with a circular shape of the edge cross-section and predicts that at certain chemical compositions a pore can be stabilized. This might explain the existence of so-called nonconducting prepores and metastable single pores in lipid bilayers reported in Melikov et al. (2001).

The model of the stress free stalk essentially uses the concept of spontaneous curvature, and it predicts how the variation of this parameter would influence different stages of the process. This question was at the center of attention of numerous experimental studies of membrane fusion (see Review in Chernomordik et al., 1995b and references therein). Their results confirm the general prediction of the model that increasing the negative curvature of both monolayers helps fusion. Just for one example, Basanez et al. (1998) demonstrated that symmetrically distributed arachidonic acid, which increases the negative curvature, enhances lipid and content mixing, and the opposite was found with symmetrically distributed lysophosphatidylcholine or palmitoylcarnitine, which facilitate a positive monolayer curvature.

The new model of membrane fusion should have important bearings on a number of other issues. Among them is the interpretation of lamellar-to-hexagonal or cubic thermotropic phase transition (Siegel, 1999) because it changes the energetic relationship between different intermediates of this process. Again the notion of spontaneous curvature plays an important role here. In the paper cited above (Basanez et al., 1998), it was shown that all lipids that facilitate fusion decrease the transition temperature, whereas fusion inhibitors increase the transition temperature. Moreover, fusion (content mixing) rates showed a maximum at the lamellar-to-isotropic transition temperature. These observations suggest that similar lipid structures are involved both in the inverted cubic phases and in membrane fusion.

The model also underscores the significance of proteins, which influence membrane curvature in biological fusion events. For example, two enzymes, endophilin (Schmidt et al., 1999) and CtBP/BARS (Weigert et al., 1999), can promote negative curvature by virtue of their abilities to convert lysophosphatidic acid, a cone-shaped lipid, into phosphatidic acid, an inverted cone. These proteins were found to be essential for vesiculation at the plasma membrane and the Golgi apparatus, respectively. We are currently analyzing the interplay between dynamin, a force generating enzyme that interacts with phosphoinositides (Barylko et al., 1998; Achiriloaie et al., 1999) and physically induces membrane bending (Hinshaw, 2000) and endophilin, with which it binds directly (Binns, Markin, and Albanesi, manuscript in preparation). In addition, we are exploring the role of other enzymes that are likely to influence membrane curvature, particularly a phospholipases A_2 enriched in secretory vesicle membranes (Hildebrandt and Albanesi, 1991).

The model of the stress-free stalk presented here, although much more advanced than the original one, still includes a number of simplifications and can be improved in some points. For example, we have rigorously calculated the shape of a monolayer stalk and found its absolute minimum when its total curvature is constant over the total area of the stalk and equal to spontaneous curvature. Clearly, the energy of the stalk cannot be made lower. When analyzing the shape of a bilayer after complete fusion (fusion pore) we used the same idea of constant total curvature of the reference surface of the bilayer. This permitted a drastic reduction in the bending energy of the bilayer, although the existence of the energy minimum was not strictly proven. More detailed analysis showed (unpublished results) that the optimum shape of a bent bilayer should be found by minimizing local energy density as a function of two principal curvatures and the energy can be somewhat decreased. However the results practically coincide with the assumption of constant curvature, at least for the bilayer without spontaneous curvature. Some modest corrections can be expected for monolayers with high spontaneous curvature and for strongly asymmetric bilayers. We shall deal with this in a separate publication (manuscript in preparation).

Gaussian curvature and corresponding bending energy was customarily neglected in majority of papers dealing with membrane transformations. There are good reasons for that especially because its elastic modulus is virtually unknown. However, in the intermediates with low bending energy the role of Gaussian component might become important, and it might need to be taken into account. Another point of concern is Helfrich's original assumption (Helfrich, 1973) that bending energy is described by a quadratic approximation. The huge success of the Helfrich model in different fields partially justifies the wide use of this approximation. However, at very small radii of curvature this approximation becomes questionable and in the future it might be revisited. For this one would need a new Hamiltonian that has not yet been developed.

Another field for improvement is the relationship between height, L, and width, b, of the stalk; in the present analysis they were allowed to acquire any value leading to the minimum of the stalk energy. We have not assumed any limitation or relationship between them. In practice there might be some limitations. For example in the presence of a "scaffold" around the fusion area (Nanavati et al., 1992; Monck and Fernandez, 1996) the degree of freedom of any one of these parameters can be limited and progress of fusion can be slowed down or even completely aborted. This would result in the well-known phenomenon of exocytosis interruptus or kiss-and-run mechanism in exocytosis (Schneider, 2001).

One more point of concern is that different contributions to the hemifusion energy were calculated separately without global minimization. That means that the total energy, although drastically reduced in comparison with the original model, might be decreased even more if different components were permitted to compensate for each other. However we do not expect this decrease to be very significant, although it remains to be demonstrated.

All of these examples show that there are many issues in membrane fusion that still need to be addressed. The theory of this phenomenon has remained a hot topic for more than a decade and is still far from completion. All the fusion intermediates that were considered by different authors essentially represent a static view of the complex multistage process. A very important understanding of transitions between these stages is still missing. There is a need of a new and different approach to this phenomenon. An important insight into this transitive process may come from the molecular dynamics modeling of membrane fusion that was recently undertaken (Ohta-Iino et al., 2001) but is still in its initial stages.

In conclusion we would like to thank L. V. Chernomordik, Yu. A. Chizmadzhev, A. J. Hudspeth, P. I. Kuzmin, and R. P. Rand for useful discussion.

Support was received from NIH grant GM55562 (to J.P.A.).

REFERENCES

Achiriloaie, M., B. Barylko, and J. P. Albanesi. 1999. Essential role of the dynamin pleckstrin homology domain in receptor-mediated endocytosis. *Mol. Cell Biol.* 19:1410–1415.

Barylko, B., D. Binns, K. M. Lin, M. A. Atkinson, D. M. Jameson, H. L. Yin, and J. P. Albanesi. 1998. Synergistic activation of dynamin GTPase by Grb2 and phosphoinositides. *J. Biol. Chem.* 273:3791–3797.

Basanez, G., F. M. Goni, and A. Alonso. 1998. Effect of single chain lipids on phospholipase C-promoted vesicle fusion: a test for the stalk hypothesis of membrane fusion. *Biochemistry.* 37:3901–3908.

Burger, K. N. 2000. Greasing membrane fusion and fission machineries. *Traffic.* 1:605–613.

Chernomordik, L. 1996. Non-bilayer lipids and biological fusion intermediates. *Chem. Phys. Lipids.* 81:203–213.

Chernomordik, L., A. Chanturiya, J. Green, and J. Zimmerberg. 1995a. The hemifusion intermediate and its conversion to complete fusion: regulation by membrane composition. *Biophys. J.* 69:922–929.

Chernomordik, L., M. M. Kozlov, and J. Zimmerberg. 1995b. Lipids in biological membrane fusion. *J. Membr. Biol.* 146:1–14.

Chernomordik, L. V., E. Leikina, V. Frolov, P. Bronk, and J. Zimmerberg. 1997. An early stage of membrane fusion mediated by the low pH conformation of influenza hemagglutinin depends upon membrane lipids. *J. Cell Biol.* 136:81–93.

Chernomordik, L. V., S. I. Sukharev, S. V. Popov, V. F. Pastushenko, A. V. Sokirko, I. G. Abidor, and Y. A. Chizmadzhev. 1987. The electrical breakdown of cell and lipid membranes: the similarity of phenomenologies. *Biochim. Biophys. Acta.* 902:360–373.

Chizmadzhev, Y. A., F. S. Cohen, A. Shcherbakov, and J. Zimmerberg. 1995. Membrane mechanics can account for fusion pore dilation in stages. *Biophys. J.* 69:2489–2500.

Chizmadzhev, Y. A., D. A. Kumenko, P. I. Kuzmin, L. V. Chernomordik, J. Zimmerberg, and F. S. Cohen. 1999. Lipid flow through fusion pores connecting membranes of different tensions. *Biophys. J.* 76:2951–2965.

Chizmadzhev, Y. A., P. I. Kuzmin, D. A. Kumenko, J. Zimmerberg, and F. S. Cohen. 2000. Dynamics of fusion pores connecting membranes of different tensions. *Biophys. J.* 78:2241–2256.

Clague, M. J., C. Schoch, L. Zech, and R. Blumenthal. 1990. Gating kinetics of pH-activated membrane fusion of vesicular stomatitis virus with cells: stopped-flow measurements by dequenching of octadecylrhodamine fluorescence. *Biochemistry.* 29:1303–1308.

Deuling, H. J., and W. Helfrich. 1977. Theoretical explanation for myelin shapes of red blood cells. *Blood Cells.* 3:713–720.

Frolov, V. A., M. S. Cho, P. Bronk, T. S. Reese, and J. Zimmerberg. 2000. Multiple local contact sites are induced by GPI-linked influenza hemagglutinin during hemifusion and flickering pore formation. *Traffic.* 1:622–630.

Fuller, N., and R. P. Rand. 2001. The influence of lysolipids on the spontaneous curvature and bending elasticity of phospholipid membranes. *Biophys. J.* 81:243–254.

Gingell, D. and I. Ginsberg. 1978. Problems in the physical interpretation of membrane interaction and fusion. *In* Membrane Fusion. G. Poste and G. L. Nicholson, editors. Elsevier, Amsterdam. 791–833.

Goni, F. M., and A. Alonso. 2000. Membrane fusion induced by phospholipase C and sphingomyelinases. *Biosci. Rep.* 20:443–463.

Hamm, M. and M. M. Kozlov. 2000. Elastic energy of tilt and bending of fluid membranes. *Eur. Phys. J.* 3:323–335.

Helfrich, W. 1973. Elastic properties of lipid bilayers: theory and possible experiments. *Z. Naturforsch. C.* 28:693–703.

Hildebrandt, E. and J. P. Albanesi. 1991. Identification of a membrane-bound, glycol-stimulated phospholipase A2 located in the secretory granules of the adrenal medulla. *Biochemistry.* 30:464–472.

Hinshaw, J. E. 2000. Dynamin and its role in membrane fission. *Annu. Rev. Cell Dev. Biol.* 16:483–519.

Hui, S. W., T. P. Stewart, L. T. Boni, and P. L. Yeagle. 1981. Membrane fusion through point defects in bilayers. *Science.* 212:921–923.

Jahn, R. and T. C. Sudhof. 1999. Membrane fusion and exocytosis. *Annu. Rev. Biochem.* 68:863–911.

Kozlov, M. M., S. L. Leikin, L. V. Chernomordik, V. S. Markin, and Y. A. Chizmadzhev. 1989. Stalk mechanism of vesicle fusion: intermixing of aqueous contents. *Eur. Biophys. J.* 17:121–129.

Kozlov, M. M. and V. S. Markin. 1983. [Possible mechanism of membrane fusion]. *Biofizika.* 28:242–247.

Kuzmin, P. I., J. Zimmerberg, Y. A. Chizmadzhev, and F. S. Cohen. 2001. A quantitative model for membrane fusion based on low-energy intermediates. *Proc. Natl. Acad. Sci. U.S.A.* 98:7235–7240.

Lee, J. and B. R. Lentz. 1998. Secretory and viral fusion may share mechanistic events with fusion between curved lipid bilayers. *Proc. Natl. Acad. Sci. U.S.A.* 95:9274–9279.

Leikin, S. L., M. M. Kozlov, L. V. Chernomordik, V. S. Markin, and Y. A. Chizmadzhev. 1987. Membrane fusion: overcoming of the hydration barrier and local restructuring. *J. Theor. Biol.* 129:411–425.

Mackintosh, F. C. and T. C. Lubensky. 1991. Orientational order, topology, and vesicle shape. *Phys. Rev. Lett.* 67:1169–1172.

Markin, V. S. and A. J. Hudspeth. 1993. To fuse or not to fuse? *Biophys. J.* 65:1752–1754.

Markin, V. S., M. M. Kozlov, and V. L. Borovjagin. 1984. On the theory of membrane fusion: the stalk mechanism. *Gen. Physiol. Biophys.* 3:361–377.

Markin, V. S., D. L. Tanelian, R. A. Jersild, Jr., and S. Ochs. 1999. Biomechanics of stretch-induced beading. *Biophys. J.* 76:2852–2860.

May, S. 2000. Protein-induced bilayer deformations: the lipid tilt degree of freedom. *Eur. Biophys. J.* 29:17–28.

Melikov, K. C., V. A. Frolov, A. Shcherbakov, A. V. Samsonov, Y. A. Chizmadzhev, and L. V. Chernomordik. 2001. Voltage-induced nonconductive pre-pores and metastable single pores in unmodified planar lipid bilayer. *Biophys. J.* 80:1829–1836.

Melikyan, G. B., S. A. Brener, D. C. Ok, and F. S. Cohen. 1997. Inner but not outer membrane leaflets control the transition from glycosylphosphatidylinositol-anchored influenza hemagglutinin-induced hemifusion to full fusion. *J. Cell Biol.* 136:995–1005.

Melikyan, G. B., R. M. Markosyan, M. G. Roth, and F. S. Cohen. 2000. A point mutation in the transmembrane domain of the hemagglutinin of influenza virus stabilizes a hemifusion intermediate that can transit to fusion. *Mol. Biol. Cell.* 11:3765–3775.

Monck, J. R. and J. M. Fernandez. 1994. The exocytotic fusion pore and neurotransmitter release. *Neuron.* 12:707–716.

Monck, J. R. and J. M. Fernandez. 1996. The fusion pore and mechanisms of biological membrane fusion. *Curr. Opin. Cell Biol.* 8:524–533.

Nanavati, C., V. S. Markin, A. F. Oberhauser, and J. M. Fernandez. 1992. The exocytotic fusion pore modeled as a lipidic pore. *Biophys. J.* 63:1118–1132.

Neumann, E. and S. Kakorin. 2000. Electroporation of curved lipid membranes in ionic strength gradients. *Biophys. Chem.* 85:249–271.

Norris, V. and D. J. Raine. 1998. A fission-fusion origin for life. *Orig. Life Evol. Biosph.* 28:523–537.

Oberhauser, A. F., J. R. Monck, and J. M. Fernandez. 1992. Events leading to the opening and closing of the exocytotic fusion pore have markedly different temperature dependencies: kinetic analysis of single fusion events in patch-clamped mouse mast cells. *Biophys. J.* 61:800–809.

Ohta-Iino, S., M. Pasenkiewicz-Gierula, Y. Takaoka, H. Miyagawa, K. Kitamura, and A. Kusumi. 2001. Fast lipid disorientation at the onset of membrane fusion revealed by molecular dynamics simulations. *Biophys. J.* 81:217–224.

Razinkov, V. I., and F. S. Cohen. 2000. Sterols and sphingolipids strongly affect the growth of fusion pores induced by the hemagglutinin of influenza virus. *Biochemistry.* 39:13462–13468.

Schmidt, A., M. Wolde, C. Thiele, W. Fest, H. Kratzin, A. V. Podtelejnikov, W. Witke, W. B. Huttner, and H. D. Soling. 1999. Endophilin I mediates synaptic vesicle formation by transfer of arachidonate to lysophosphatidic acid. *Nature.* 401:133–141.

Schneider, S. W. 2001. Kiss and run mechanism in exocytosis. *J. Membr. Biol.* 181:67–76.

Siegel, D. P. 1993. Energetics of intermediates in membrane fusion: comparison of stalk and inverted micellar intermediate mechanisms. *Biophys. J.* 65:2124–2140.

Siegel, D. P. 1999. The modified stalk mechanism of lamellar/inverted phase transitions and its implications for membrane fusion. *Biophys. J.* 76:291–313.

Stegmann, T. 2000. Membrane fusion mechanisms: the influenza hemagglutinin paradigm and its implications for intracellular fusion. *Traffic.* 1:598–604.

Volkov, A. G., D. W. Deamer, D. L. Tanelian, and V. S. Markin. 1998. Liquid interfaces in chemistry and biology. John Wiley & Sons, New York.

Weigert, R., M. G. Silletta, S. Spano, G. Turacchio, C. Cericola, A. Colanzi, S. Senatore, R. Mancini, E. V. Polishchuk, M. Salmona, F. Facchiano, K. N. Burger, A. Mironov, A. Luini, and D. Corda. 1999. CtBP/BARS induces fission of Golgi membranes by acylating lysophosphatidic acid. *Nature.* 402:429–433.

Zimmerberg, J. 2000. Are the curves in all the right places? *Traffic.* 1:366–368.

Zimmerberg, J. and L. V. Chernomordik. 1999. Membrane fusion. *Adv. Drug Deliv. Rev.* 38:197–205.